NASA Major Volcanic Eruption Response Plan

Version 11, 1 March 2018

1. Executive Summary

- A major volcanic eruption would severely impact climate and life on Earth. NASA's research tools provide the capability to give a first order estimate of this impact for policymakers and the global community. NASA's research tools include satellites, balloons, ground-based instruments, aircraft, and modeling capabilities. To optimize the use of these tools, we have devised a rough plan of action that can be quickly implemented following such an eruption.

- The first step in the development of this mission deployment plan was a 2-day NASA-headquarters-sponsored workshop (17-18 May 2016). The objective of this workshop was to draft deployment plans, which include an assessment of how significant an eruption needs to be before a deployment effort is needed, answerable science questions, measurement requirements for those questions, satellite and sub-orbital platform requirements, and proposed deployment timelines.

- The workshop participants determined a radiative forcing of -1 Wm^{-2} requires an injection of about 4-6 Mt of SO_2. Hence, an SO_2 injection into the stratosphere of ~5 Mt or greater has sufficient climate impact to warrant the use of significant resources.

- NASA should pre-establish an early response team (ERT) of a few scientists and managers to ensure that the proper personnel and assets have been tabulated, and plans for individual NASA assets have been detailed and are at least in place. This ERT should also update this plan on an annual to bi-annual basis.

The NASA response to a major eruption begins with the identification of team leads. The leads are tasked with insuring that their contacts to the NASA tools are in place and capable of responding to a science call following an eruption. These leads include:

1. HQ volcano response program scientist
   a. Early Response Team (ERT)
2. Program manager
3. Project Scientist(s)
   a. Satellite lead
   b. Modeling lead
   c. Ballooning lead
      i. Small balloons
      ii. Heavy lift
   d. Aircraft lead
      i. High Altitude
      ii. Heavy lift
   e. Ground lead
      i. Lidars: MPLNET, NDACC
      ii. Aerosol: AERONET
      iii. Chemistry: Dobson/Brewer/Pandora

A rapid response to a major volcanic eruption requires fast initial movement because the plumes evolve from SO_2 to aerosol on a time scale of less than one month, and the processes of self-lofting, dispersion, and sedimentation out of the stratosphere take place on time scales of days to months to years, respectively. The first month is especially crucial to determine the spread of the plume in altitude and the total amount of gas (SO_2 and other gases) injected, to observe rapid SO_2 removal on ash or ice and the gas-to-particle processes, and to quantify possible direct injection of halogens to the stratosphere. Figure 1 displays a flow chart of the NASA response, beginning with the eruption detection to the field campaigns.

The volcanology community already provides early alerts to potential eruptions through several channels. The Smithsonian's *Global Volcanism Program* and the *Volcanic Ash Advisory Centers* (VAAC) track and publicly alert imminent and ongoing eruptions. The *volcanicclouds* Yahoo email list provides near real time information about dispersing volcanic clouds from on-going eruptions is discussed by volcanologists, meteorologists, pilots, and satellite remote sensing experts. Example posts include ash retrievals from the operational geostationary satellites.

- Rapid scan VIS loops from geostationary satellites
- Quick volcanic cloud dispersion forecasts
- Aerosol and SO_2 maps from hyperspectral UV, VIS and NIR LEO satellites,
- CALIOP "curtains"

The timeline of the initial response would be:
- Day –n: Volcano observatories (via WOVO and VAACs) communicate raised alert levels, and inform if past record and current knowledge of eruptive potential makes significant eruption of a volcano likely within n±y days.
- Day 0:   Eruption occurs
- Day 1:   Once satellite scientists verify a major eruption, HQ ERT meets for initial plan and final decisions on asset lead scientist selections. Preliminary model simulations are initialized to aid with initial mission planning.
- Day 3:   ERT and lead scientists meeting to establish the following:
    o Whether the event represents a major eruption, based on satellite data and initial model simulations;
    o Potential supplemental mission questions, goals, and priorities;
    o Initial mission plan;
    o Available assets, preliminary cost estimate, and reporting plan;
    o Briefing of stakeholders (i.e., program managers, Science Mission Directorate leadership).
- Day 3:   Asset teams are contacted to re-task the available assets.
- Day 6:   The initial revisions to the plan by the ERT are agreed upon (depending on the specifics of the eruption evolution), and model simulations refined after new initialization estimates.

The flow chart for the volcanic response plan evolves from the first notification of the eruption to the final flights observing the volcanic cloud. The initial meeting on Day 1 (see

above) would involve HQ, satellite scientists, and the Project Scientists (as chosen by HQ). This small group would decide whether to trigger a full response to an eruption. If so, model simulations would be initiated and a full team meeting would be convened on Day 3. The flow chart of the plan is shown below.

Volcano Rapid Response Flow Chart
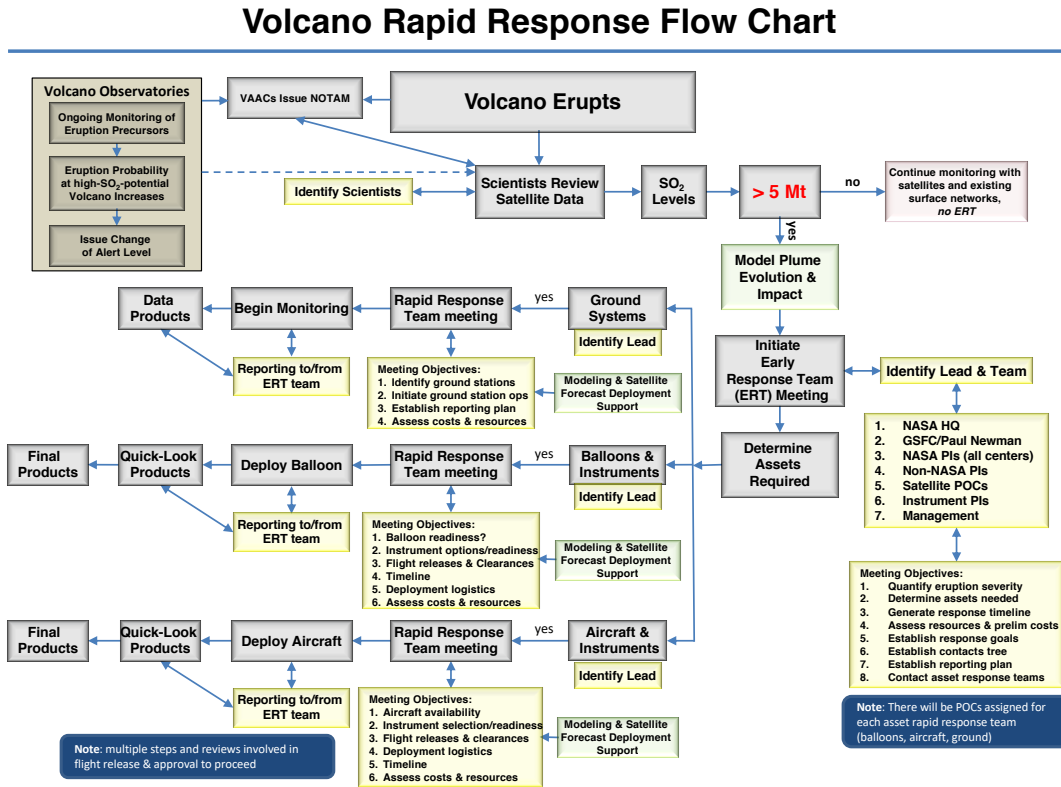
Figure 1: Volcanic rapid response flow chart. Grey boxes indicate team actions, yellow boxes show meetings or meeting actions, green boxes are for modeling activities. Tan box (top left) shows Volcanic Ash Advisory Center (VAAC) activities outside of NASA.

The specific plans for NASA's assets are detailed in sections below. These plans provide a near-term response (< 1-2 months), and a long-term response (1-2 years). The initial plan is to provide a quick appraisal of the volcanic impact for US policymakers within a week of the eruption. Observations over the first month will constrain and refine this appraisal, and subsequent observations will provide key inputs for answering science questions.

2.   Preface

An eruption with emissions the same scale as the 1991 Mt. Pinatubo volcanic eruption (15-20 Mt SO_2) would have a major impact on both climate and stratospheric ozone concentrations for a multi-year period. Recent work has revealed that smaller eruptions that inject material into the stratosphere may also have important effects on both climate and ozone. However, the Pinatubo-scale eruption is the subject of this report.

NASA has traditionally led the investigations of eruptions causing stratospheric injections because of their major investments in atmospheric aerosol and chemical observations, their global observation capabilities with satellites, and their unique suborbital assets for measuring the evolution of the volcanic clouds in the stratosphere.

To **understand the impact of eruptions on the stratosphere and surface climate**, we have developed a mission deployment plan.

The NASA plans for a major volcanic eruption involve three essential questions:

- Over 60 volcanic eruptions occur every year among ~450 active volcanoes. How can we determine if an eruption merits extensive studies and what would we do if another Pinatubo-sized eruption occurred?
- Based on observations after historical events and current volcano science studies, what do we expect to occur after future eruptions and what questions are important to resolve through measurements after future eruptions?
- What key information is needed from current NASA assets, and which platforms are needed, to obtain the observations required to understand how volcanic eruptions impact weather, climate and atmospheric chemistry?

This report documents a NASA plan to be implemented only in the event of a major eruption. We will not use this plan at the present moment to start the approval process for any particular observations, but the plan does identify impediments and preparatory actions to ensure a timely response. While this plan is NASA-centric, it becomes a starting point for partnering with other US federal agencies and the international community to define a global science implementation plan. No funding is currently available for this plan. If a volcanic eruption occurs, the emergency funding will depend on the scale of the eruption, and the ability to identify funds within the existing Earth Science program.

The overall plan depends on the availability of satellite, ground, and suborbital observations. These measurements will be needed to quantitatively test hypotheses and project the evolution of climate and stratospheric ozone. These projections will provide a solid basis for informing policy makers and the public on the volcanic impact. This report prioritizes observations among the sampling platforms with respect to both the capabilities of the platforms, and the ability of measurements from them to answer science questions.

3.   Introduction

O. Brian Toon, Paul Newman, Alan Robock, Florian Schwandner

The eruption of Mount Pinatubo in June 1991 demonstrated the dramatic impact of volcanic gases and particles on humans and the environment. Some much larger eruptions could be devastating to modern society worldwide, but these are fortunately rare (Newhall et al., 2018). NASA observations and research, as well as those of others, showed that the Pinatubo cloud led to both surface cooling and ozone depletion. Because of such dramatic impacts, NASA needs to be prepared to provide information to the public and policy makers on the effects of another Pinatubo-scale eruption. It is important that NASA measure the properties of rapidly evolving volcanic clouds and the response of the climate and atmospheric chemistry to them. The purpose of this document is to provide a basic plan for responding to such an eruption.

3.1. Key challenge: Understanding the impact of volcanic eruptions on climate and atmospheric chemistry

Volcanic clouds have a number of impacts (Robock, 2000). Stratospheric hazes of sulfate aerosols originating from the volcanic sulfur dioxide (SO_2) emission have been observed to scatter sunlight back toward space, reducing the Earth's radiative heating and cooling the surface and the troposphere. This cooling reduces atmospheric water vapor and precipitation. The volcanic hazes are primarily composed of sulfate aerosols that form from the volcanic emissions of SO_2. These sulfate aerosols also absorb sunlight and terrestrial radiation, heating the stratosphere and leading to stratospheric dynamical changes, spreading the volcanic aerosols in latitude more quickly and more extensively than would occur without it. Heterogeneous chemical reactions that occur on volcanic cloud particles alter stratospheric chemistry and lead to changes in ozone concentrations.

Table 1. Observed changes in climate and chemistry after eruptions

Observed	Probable cause
Cooling troposphere and surface	Reduction in shortwave forcing by aerosol
Ozone loss / enhanced surface UV	Heterogeneous reactions on sulfate aerosols
Tropopause and stratospheric warming	Sunlight and IR absorption by aerosol
Mid-latitude NH winter warming	Stratosphere/troposphere dynamical interaction
Rapid spread of volcanic clouds	Alteration of atmospheric dynamics
Hazy skies / bright twilights / reduction in shortwave at surface	Scattering by aerosols
Enhanced diffuse radiation at surface/ enhanced CO_2 sink	Scattering by aerosols
Increase in stratospheric ClO; decrease in stratospheric NO_2	Heterogeneous reactions on sulfate aerosols
Change in stratospheric CH_4, H_2O	Change in dynamics and tropopause temperature
Change in tropospheric CO_2, CO, CH_4	Changes tropospheric UV levels, drop in sea surface temperature
Reduction in water vapor column	Sea and land surface cooling
Reduction in global average precipitation	Reduction of solar heating of sea surface
Expected	
Cirrus cloud increase/decrease	Seeding by large sulfate particles
Cooler days	Loss of sunlight
Cooler nights	Loss of sunlight, little IR change
Polar amplification	Decreased poleward energy flux
Increase in sea ice	Polar cooling

Observations of the form, structure, composition, and temporal evolution of volcanic clouds are crucial to quantify the perturbation to the Earth's system, but observations of the system's response are equally important for quantifying the impact of these clouds. Observations of climate and chemistry perturbations are important not only because of their potential impacts on the Earth, but also because they teach us about how the atmosphere works, serve as tests of Earth system models, provide analogs of stratospheric aerosol geoengineering and test the climate sensitivity to perturbations to the Earth's radiation budget. During the past decade advances in measurements and analysis techniques have allowed the science community to measure the perturbations to surface, tropospheric, and stratospheric temperatures, clear-sky shortwave radiation, atmospheric water vapor, and precipitation (see Table 1) following injections of volcanic material into the stratosphere by eruptions much smaller than Pinatubo. These injections produce radiative forcing, which contributes to climate change, and can impact the Antarctic ozone hole. Given the intense focus on climate change it is increasingly important to be able to disentangle natural from human-driven forcing on climate.

Table 2. Particle properties that need to be determined as functions of time and space

Particle properties to measure	Possible ranges
Composition	Dust, ash, sulfates
Size distribution	nm to tens of microns
Number	nm to tens of microns
Mass	
Shape (spheroid aspect ratio)	0.1 to 10
Optical constants	refractive indices
Extinction optical depth	0.001 to 10
Scattering optical depth	0.001 to 10
Absorption optical depth	0.001 to 1
Scattering phase function	

Table 3. Gases that need to be measured

Gas to measure	Purpose
SO_2	Need to constrain cloud mass
H_2S, other injected sulfur gases, CS_2, COS	Need to constrain injection composition
H_2SO_4, other sulfur cycle components	Need to close sulfur cycle
Water vapor	May be a significant perturbation to the stratosphere
HCl, other injected gases with halogens, N	Quantify injections of ozone destroying species
Components of O_3 catalytic cycles	Understand perturbed chemistry
Tracers	Useful to examine altered dynamics

Models simulating volcanic aerosol effects on climate have advanced in the past decade. Some are now capable of tying together the complex evolution of atmospheric chemistry, particle microphysics, radiative forcing and climate changes that occur after eruptions. The initialization of these models is crucially dependent on the details of the particular eruption, for example its timing and location, the amount of sulfur dioxide (SO_2), water, and halogens (such as HCl) injected, as well as the state of the system at the time of the eruption, for example the phase of the Quasi-biennial Oscillation (QBO) and of El Niño Southern Oscillation (ENSO). New observations from aircraft, balloon and satellite measurements have now expanded our

capability to measure the system's components required to correctly initialize models, as well as those properties needed to evaluate them.

Taken together, advances in measuring the atmospheric state, gases, and aerosols, as well as in modeling aerosols and their effects on climate and chemistry, will allow us to evaluate the impact of the next major volcanic eruption. This, however, will only be possible if we are well prepared to act in a timely manner following the eruption.

3.2.   Required observations of volcanic clouds

The complexity of volcanic impacts on climate and chemistry requires that a large number of particulate and gaseous species be measured (Table 2 and

Table 3). The quantification of climate impacts require the measurement of optical particle properties in addition to composition, size distribution, and number density. The size of the eruption is estimated by the measurement of SO_2 but for closing the sulfur cycle, other sulfur compounds need to be measured. Volcanic gases contain halogen and nitrogen-bearing species (Delmelle and Stix 2000, Schwandner et al. 2013) that may have a significant impact on the stratospheric ozone layer if injected into the stratosphere (McCormick et al. 1995). In addition, the hot plume environment and the availability of surfaces for heterogeneous chemistry enable the chemical conversion of species of both volcanic and atmospheric origin (Mather 2008), such that a broad characterization of the chemical environment is required. All *major* (O_3, H_2O, CO_2, SO_2) and *minor* (HDO, CO_2, SO_2, CO, CH_4, HO_x, ClO_x, BrO_x) volcanic gas species should be measured for full chemical characterization of the source term for chemical conversion modeling.

The odds of a volcanic eruption such as that of Pinatubo in 1991, whose stratospheric cloud was able to force the climate at more than –1 W m^{-2}, are about 3% in a given year. Few eruptions occur with little or no warning (Winson et al. 2014). In most cases of the past 40 years, including Pinatubo in 1991, volcano observatories have provided days to weeks of warning as raised alert levels, and past history and current knowledge of the volcanological community was and can be a source of hazard potential information (Fearnley et al. 2017). Most volcanoes are located in the tropics or high latitudes, where few ground-based, balloon-borne or aircraft-borne instruments are readily available. Much of the interesting evolution occurs within a few months, but clouds persist for a couple years. These factors make satellites essential for many of the needed measurements. However, there are measurements that satellites currently cannot make, and satellite observations need to be evaluated. Therefore, aircraft-, balloon- and ground-based measurements will also be needed.

Numerous satellites are currently in orbit and making relevant measurements for volcanic eruptions (see section 6.0). Various satellite instruments are able to measure SO_2, and several instruments are able to measure the column aerosol optical depth. However, most of these are not able to vertically profile the optical depth. Nadir-viewing instruments have difficulty detecting small volcanic clouds against the background of the tropospheric aerosols. The CALIOP lidar is very valuable for high-resolution vertical information. Limb sounders such as the Canadian OSIRIS or the SUOMI OMPS limb sounder also provide useful vertical profiles of aerosols. However, these measurements are not as straightforward as those from previous solar occultation measurements from instruments such as SAGE. Distinguishing clouds from aerosols near the tropopause

challenges many space-based measurements. Moreover, after an eruption as large as those of interest for this plan the limb sounding instruments will be blinded by the high optical thickness of the aerosols along the limb and occultation instruments will saturate, as happened to SAGE II after the eruption of Mt. Pinatubo. SAGE III, now on the International Space Station, is more sensitive than SAGE II, but still may not be able to observe through thick clouds, and its orbit prohibits high latitude observations.

3.3.   Linking space-based observations with ground-, air-, and balloon-based observations.

Robust ground-based, aircraft and balloon programs are essential for augmenting satellite observations of volcanic clouds. These platforms should be used to complete our understanding of the stratospheric sulfur cycle, which has not been fully explored. They should also be used to investigate the properties of the ambient aerosol layer and its perturbations by small volcanic eruptions of the sort that occur every few years. Understanding the structure and composition of the background aerosols is necessary in order to understand how volcanoes perturb that layer. For example, many assume that the aerosols above the tropopause are sulfuric acid. However, recent data and models indicate that organic aerosols are a significant fraction of the background aerosol up to about 20 km altitude, which is well above the tropopause.

The first step in this program should be development, testing, and evaluation of the instruments that are currently available to address the relevant issues in **Error! Reference source not found.**, Table 2, and

Table 3. The second step should be to setup a rapid response program (~2 weeks) for satellite instruments, ground-based networks, and small balloons, to allow timely measurements of emissions from small volcanic eruptions. Aircraft measurements should be directed to the later stages (1-2 months up to a few years) of volcanic cloud evolution for large eruptions. A plan should be set up to enable a relatively quick response using NASA aircraft once a large eruption is identified. This plan will require that new instruments be developed and tested in advance.

4.   Criteria for NASA response to volcanic eruption

The mass of sulfur dioxide (SO_2) injected into the stratosphere by an eruption is the most appropriate criterion to identify the climate relevance of a volcanic injection. SO_2 is measured by numerous satellites, has a 35-year history of being used to identify important eruptions, and has been shown in both models and observations to be predictive of which volcanic clouds will have enough aerosol optical depth to modify the climate. For example, the Mt. St. Helens eruption of 1980 was a very powerful energy release, but produced little stratospheric SO_2 and had no significant effect on climate (Robock, 1981). Generally, the SO_2 mass injected into the stratosphere can be determined within a few days of an eruption with reasonable accuracy.

In the past 35 years only two years had stratospheric injections from all eruptions greater than or equal to 10 Mt of SO_2, 1982 and 1991 (see Figure 2). In 1982, El Chichón injected ~7 Mt SO_2 and several small eruptions ~2 Mt cumulatively, and in 1991 Mt

Pinatubo injected ~14-18 Mt (with the total amount still not yet well quantified) and Cerro Hudson an additional 4 Mt. Six individual years had smaller eruptions that injected in the atmosphere between 1 and 4 Mt SO_2, but those injections may not have been in the stratosphere. For example, the 2011 eruption of Nabro, Eritrea injected about 4-5 Mt in the atmosphere (Figure 2), of which only ~2 Mt in the stratosphere (Table 4).

The maximum optical depth from volcanic aerosols and the associated radiative forcing are also a good metric for quantifying major volcanic events, albeit they are reached only months after the eruption. Table 4 provides some estimates of the global average optical depth, radiative forcing, and SO_2 emitted by several volcanic eruptions from 1902 to 1992. Radiative forcings are estimated assuming that the forcing per unit optical depth is -25 W m^{-2}. Many of these volcanic clouds were isolated primarily to only one hemisphere (Mt. Agung, El Chichón), and some to high latitudes in one hemisphere (Katmai). SO_2 data only exist since about 1980. If we establish the threshold for a large

Table 4. Properties of some of the largest volcanic SO_2 eruptions of the past century.

Volcanic eruption	Year	Global optical depth Source	Estimated RF, Wm^{-2}	SO_2 (Mt) Carn et al. (2015)**
Well above tropopause		*Sato**		
La Soufriere, Santa Maria	1902	0.08	–2	
Novarupta (Katmai)	1912	0.04	–1	
Mt. Agung	1963	0.09	–2.25	
Mt. Fuego	1974	0.04	–1	
El Chichón + others	1982	0.1	–2.5	8 (+2)
Mt. Pinatubo	1991	0.15	–3.75	18
Near tropopause		*Santer***		
Cerro Hudson	1991			4
Misc.	2006	~0.003		0.8
Kasatochi	2008		~ –0.025	2
Sarachev	2009	~0.002		1.2
Nabro	2011	~0.003	~ –0.04	2

* http://data.giss.nasa.gov/modelforce/strataer/tau.line_2012.12.txt

** https://disc.gsfc.nasa.gov/datasets/MSVOLSO2L4_V2/summary?keywords=SO2

*** Read from graph in Santer et al. (2015)

eruption as a radiative forcing of -2 W m^{-2}, comparable in magnitude to that of greenhouse gases since the start of the industrial era, 4 years (1902, 1963, 1982 and 1991) show a volcanic radiative forcing exceeding this threshold. Of course, these volcanic perturbations do not last long enough to overcome the ocean thermal response time and realize their full impacts on the global climate system. There are two other years (1912 and 1974) when the radiative perturbation may have been -1 W m^{-2}.

Scaling using the 1982 annual injection of 10 Mt of SO_2, mostly from El Chichón, and the 1991 annual injection of 22 Mt of SO_2, mostly from Pinatubo, indicates that a -1 W m^{-2} forcing requires an injection of about 4-6 Mt of SO_2. The difference between 4 and
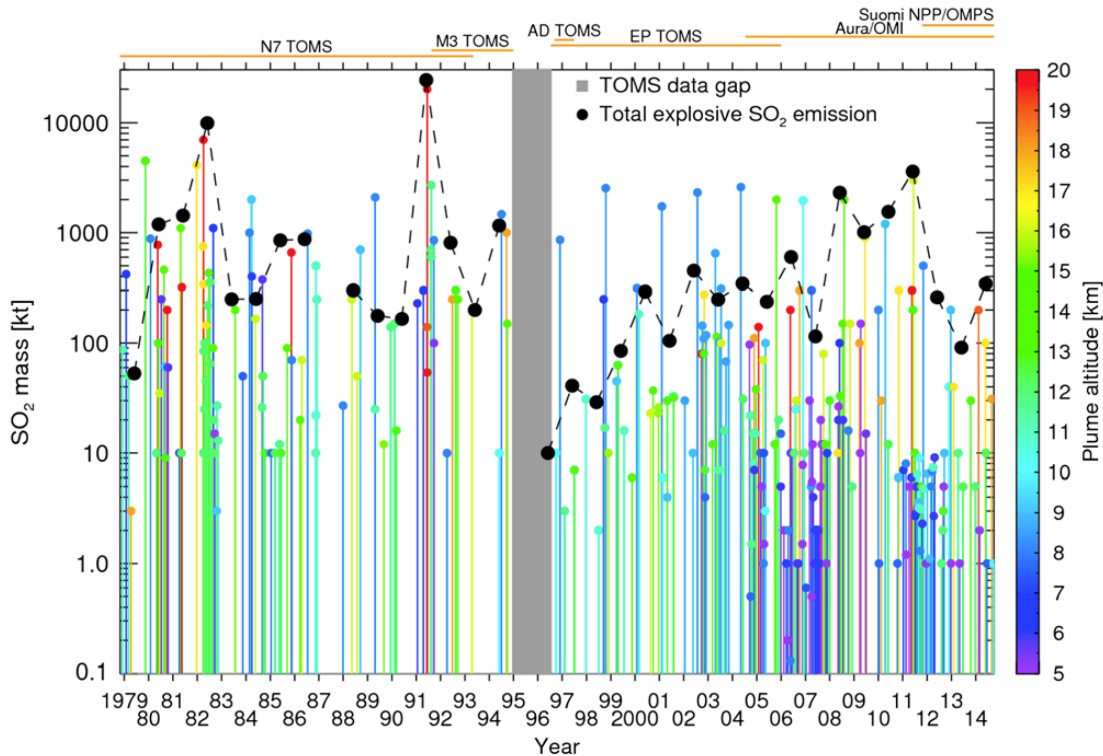
Figure 2. UV satellite measurements of volcanic SO₂ emissions by explosive and effusive eruptions October 1978 to October 2014 based on Total Ozone Mapping Spectrometer (TOMS), Ozone Monitoring Instrument (OMI), and Ozone Mapping and Profiler Suite (OMPS) data. Colors indicate height of injection. Black dots indicate yearly total emissions above the tropopause. Fig. 1 from Carn et al. (2015).

6 Mt in the amount of SO_2 needed for a -1 Wm^{-2} forcing lies partly in the difficulty of using a global average optical depth for volcanic clouds, which are not uniform over the Earth, to estimate the forcing. Radiative forcing is not expected to be linear in SO_2 because forcing depends on particle size in addition to mass injected, so larger injections are less effective per unit mass than smaller ones. In addition, some of the SO_2 first converted to sulfate is lost on large ash particles in the first few weeks following the eruption, and likely leads to little radiative forcing.

An SO_2 injection into the stratosphere of 5 Mt or greater has sufficient climate impact to warrant the use of significant resources. On the other hand, even a smaller eruption, if located within the U.S., such as the 1980 Mt. St. Helens eruption, might warrant the deployment of significant resources. The U.S. is the most volcanically active country on Earth (followed by Russia, Indonesia and Japan), and therefore the possibility of such an eruption is not remote. Tropical, high latitude, and near tropopause eruptions may produce different spatial and temporal distributions of volcanic clouds, resulting in different climate and chemical impacts. Given our limited understanding of these different types of events, we recommend the same criterion (i.e., injection > 5 Mt SO_2) for eruptions at all latitudes.

Given this discussion we conclude that:

13

1. **Satellite observations of SO₂ provide the information necessary for deciding whether to initiate an observational and modeling plan in response to an eruption.** There are many capable satellites currently in orbit that should provide a wealth of data for eruptions large and small. For injections of SO₂ less than 1 Mt, satellite data may be all that is warranted.

2. **Eruptions emitting more than 5 Mt of SO₂ into the stratosphere warrant using aircraft and balloons as soon as possible after the eruption to augment satellite observations**, which may be obscured by volcanic emissions for UV/Vis limb sounders, and to measure variables that are not observable by satellite, such as the full particle size distribution. They would also serve to calibrate satellite observations. In the past 115 years there have been four such perturbed years (1902, 1963, 1982 and 1991).

3. **Eruptions emitting between 1 and 5 Mt of SO₂ into the stratosphere, or a cluster of such eruptions with a yearly injection of 1-5 Mt warrant using lightweight balloons to augment and verify satellite observations.** Such events occur about every 6 years, based on the data in Figure 2. There are a number of things that can be learned from eruptions smaller than 5 Mt SO₂, including: how long ash stays in the atmosphere; how sulfate might be removed on ash or on ice; and, the details of microphysical transformation of SO₂ to sulfate aerosols, including if there is an eruption into an existing sulfate cloud. These topics might be explored with aircraft as part of other missions as targets of opportunity, or with proposal based studies when opportunities arise.

5. Balloon-based observations

Ru-Shan Gao, Jean-Paul Vernier, Lars Kalnajs, Terry Deshler, Ross Salawitch

5.1. Introduction

Obtaining early information on the vertical distribution and microphysical and optical properties of a volcanic plume is crucial to forecast and understand the impacts on weather, climate, and stratospheric ozone. The next major volcanic eruption will be observed by a number of satellites, which will provide information on the vertical and horizontal distributions as well as bulk optical properties of volcanic aerosol. However, in situ measurements will be required to obtain aerosol size distribution and composition that can be used to feed satellite retrievals of volcanic aerosol properties and validate numerical dispersion models. This information has to be obtaining quickly (i.e., within the first month of the eruption) to understand early microphysical processes: the transition between ash-rich to sulfate-rich plumes, the conversion of SO₂ into sulfate and the removal of ash by sedimentation.

A balloon deployment of light-weight instruments may be mounted within the first two weeks following an eruption to make early in situ measurements of aerosol and chemical properties of a fresh plume. Flights for heavier payloads will require shipping and infrastructure, leading to delays of first flights to a few months after an eruption. Prerequisites for such a rapid deployment include prior preparation of instruments, selection of launch locations, and formulation of logistics. This section aims to provide a

list of existing instruments that can be used in a response plan following a major volcanic eruption.

5.2. Instrument assets (currently or soon available)

The University of Wyoming (UWy) has launched Optical Particle Counters (OPC) to make in situ measurements of aerosol size distribution in a number of volcanic plumes for the past 30 years, mostly from mid-latitude sites (Laramie, WY and Lauder, New Zealand) but occasionally in the tropics (Darwin, Australia) and in Antarctica. The OPCs developed by UWy are suitable to study new particle formation and differentiate ash and sulfate aerosols in a volcanic plume (Deshler et al., 2006). NASA Langley had worked with UWy to organize a balloon deployment from Darwin after the Kelud eruption, which obtained key information on the microphysical properties of volcanic aerosol (Vernier et al., 2016). While the deployment has demonstrated that such measurements can be made one month after an eruption, logistics were complex due to the large size, heavy weight, and high cost of the existing payload. Smaller, lighter and disposable aerosol payloads are needed for a quicker response.

A light-weight aerosol backscatter sonde (COBALD) developed by ETH could be used to measure the backscatter properties of volcanic aerosol with fine vertical resolution and high signal-to-noise ratio. Recently, an OPC (Printer Optical Particle Spectrometer, or POPS) suitable for aerosol particle number density and size distribution in the diameter range of 0.14 – 3 μm was developed by NOAA (Gao et al., 2016). NASA Langley has recently tested a medium weight OPC, with a 0.3 – 10 μm diameter range and aerosol impactor during balloon field campaigns in India. This medium weight OPC can be mounted under weather balloons and deployed rapidly for field missions. The University of Colorado is also downsizing the existing UWy OPC system to be mounted under weather balloons and is developing a light-weight condensation nuclei counter. Additional payloads for ozone (ozonesonde) and water vapor measurements (Cryogenic Frost point Hygrometer (CFH), Frost Point Hygrometer (FPH)) within a volcanic plume can also be deployed rapidly under weather balloons. An SO_2 measurement technique using a modified dual-ozonesonde instrument would yield very useful information if deployed in a young volcano plume (first month).

Stratospheric gases injected by the eruption and produced through chemical processing of injected gases can be measured by NASA's balloon-borne optical remote sensing payload. The MkIV (Toon, 1991) performs solar occultation spectrometry in the infrared and simultaneously measures vertical profiles of over 40 trace gases, including virtually all relevant gases in Table 3. Since 1989, 24 MkIV balloon flights have been conducted with launches in the subtropics and in the Arctic. Deployed many months after the eruption of Mt. Pinatubo, MkIV was still able to detect stratospheric chemical alterations attributed to the eruption (Toon et al., 2016). The MkIV is currently being upgraded with a new sun tracker that operates in the short-wave infrared in order to improve its performance in conditions of high aerosol loading. Also available is the Submillimeter Limb Sounder (SLS), a heterodyne radiometer that measures molecular emission spectra in limb geometry. SLS can retrieve vertical trace gas profiles, including HCl, ClO, BrO, O_3, HO_2, N_2O, and HNO_3 (Stachnik et al., 2013), and has flown on numerous flights since 1991, often sharing the balloon gondola with the MkIV. An

advantage of SLS over the MKIV is its ability to make microwave measurements in the presence of thick volcanic plumes.

Table 5. Listing of light weight aerosol, ozone and water vapor payloads which could be used for a rapid response after the next volcanic eruption. All particle measurements are in diameter.

Payloads	Institute/Contact	Specifications	Weight	Cost
POPS	NOAA/ Ru-Shan Gao	OPC, 0.14 – 3 μm, 8 – 25 channels	0.75 kg	$2K[a]
COBALD	ETH/Frank Wienhold	Backscatter at 455and 870 nm	0.6 kg	$1.6K[b]
LPC	University of Colorado/ Lars Kalnajs	OPC, 0.3 – 15 μm, 32 channels	4 kg	$6K[a]
LCN	University of Colorado/ Lars Kalnajs	Condensation Nuclei > 6 nm	2 kg	$3K[a]
LHI-PC	University of Colorado/ Lars Kalnajs	OPC with heated inlet, 0.3 – 15 μm, 32 channels	4.5 kg	$7K[a]
LOPC	NASA Langley/ Jean-Paul Vernier	OPC, 0.3 – 10 μm, 8 channels	4.2 kg	$3K[a]
LImpact	NASA Langley/ Jean-Paul Vernier	3 stages cascade aerosol impactor	4 kg	$7K[a]
CFH	ENSCI	Water vapor sonde	1 kg	$3.2K[b]
FPH	NOAA	Water vapor sonde	1 kg	x[a]
Ozonesonde	ENSCI	ozone	0.6 kg	$0.7K[b]
SO₂ sonde	St. Edward's University/ Gary Morris	SO_2, ozone	2 kg	$2K[b]
iMet	InterMet	Radiosonde, p, T, RH	0.26 kg	$0.3K[b]

[a]Built in institute, labor cost excluded, [b]Commercially available

Table 6. Listing of heavy payloads that are not disposable

Payloads	Institute/	Specifications	Weight

5.3.   Preparatory actions

5.3.1.   Balloon site selection

Nine stations, roughly evenly distributed between 40°N and 40°S have been selected for a balloon deployment with small payloads after the next major volcanic eruption (Table 7A**).** The selection gave preference to sites with aerosol lidar and balloon launch capabilities. Some of these sites are part of the Network for Detection for Atmospheric Composition Changes (NDACC).

Table 7. Selected sites for balloon deployment (A. Small payloads, B. Heavy payloads).

A. Small Payload Locations		Additional Assets	Alternatives
Boulder, CO, USA	40.0°N, 105.3°W	NDACC site - lidar, sondes, UV	Hampton, VA, USA (37.0°N, 76.5°W)
Table Mountain Observatory, CA, USA	34.4°N, 117.7°W	NDACC site - lidars, UV	Houston, TX, USA (29.8°N, 95.4°W)
Hilo, HI, USA	19.7°N, 155.1°W	NDACC site - lidar, sondes, UV	Key West, FL, USA (24.6°N, 81.8°W)
Gadanki, India	13.4°N, 79.2 °W	Aerosol Lidar	Barbados; San Jose, CR
San Cristobal, Ecuador	0.9°N, 89.4°W	Sondes (GAW regional station)	Manaus, Brazil (Lalinet Station), Nairobi, Kenya (GAW station)
Pago Pago, American Samoa	14.3°S, 170.7°W	Sondes (NOAA station)	Darwin, Australia (GRUAN station)
Reunion Island, France	21.1°S, 55.5°E	NDACC site - lidar, sondes, UV	
Buenos Aires, Argentina	34.5°S, 58.5°W	Lalinet Station, multi-wave lidar	
Lauder, New Zealand	45.1°S, 169.7°E	NDACC site - FTIR, lidars, microwave, UV	

B. Heavy Payload Locations		Remarks
Fairbanks, AK, USA	64.8°N, 147.7°W	MkIV/SLS launched previously by CSBF
Ft. Sumner, NM, USA	34.5°N, 104.2°W	Site for summer/fall launches, regular CSBF launch site, MkIV/SLS launched previously by CSBF
Daggett, CA, USA	34.8°N, 116.9°W	Site for winter/spring launches, MkIV/SLS launched previously by CSBF
Alice Springs, Australia	23.7°S, 133.9°E	Large balloon payloads launched previously by CSBF

Four launch sites have been selected for the deployment of large balloon payloads (Table 7B**).** The sites cover a latitude range from the northern high to the southern mid-latitudes. Selections were based on the suitability of facilities for launching large balloons and sufficient downwind range (~200 miles). The Columbia Scientific Balloon Facility (CSBF) has successfully launched payloads on large balloons from all of these sites.

5.3.2. Instrument preparation

Five to 10 sets of iMet/COBALD/POPS/O$_3$/SO$_2$/CFH/CN sondes should be stockpiled for rapid (0-30 days) response. We further recommend selecting a team of instrument PIs who will keep and maintain these instruments and corresponding calibration equipment and material in such conditions that they can be shipped within two days and will be ready for launch two days after arrival at the launch site.

The balloons and and their instruments should be launched regularly, every few months, to establish a background climatology that can be compared to the observations after a large eruption. These launches will also provide practice to the crews in preparation of the balloons and their instruments, and in retrieving and analyzing the data, to work out any kinks and be ready for more rapid launches when the time comes.

5.4. Near term plan (0-1 month after the eruption)

Deploy light balloon payloads within two weeks after the eruption at pre-selected sites within the same latitudinal band as the volcano, and as close as possible to the eruption location. Expand to neighboring site(s) as the plume expands latitudinally.

Notify CSBF of plans to launch the MKIV as soon as possible. Instrument selection and site selection will occur shortly after the eruption. Shipments of hardware to the selected location will require substantial time to the deployment site (particularly for a Southern Hemisphere eruption).

5.5. Long term plan (>1 month after the eruption)

We plan to continue the launch of light balloon payloads at a decreasing pace after the first month, and to maintain once-a-month launches after the first year after the eruption. We plan to increase the frequency of launches as needed in support of aircraft campaigns. Heavy payloads will also be available for launch about 1 month after the eruption. On a longer time-scale, we should be prepared to launch additional in situ and remote packages in the months and years following the eruption.

While the heavy lift balloons are extremely valuable, the costs, flight limitations, and logistics suggest that only 1-3 launches will be accomplished.

6. Satellite-based observations

R. A. Kahn (MISR, MODIS, VIIRS), P. K. Bhartia (Limb), N. Krotkov (OMI, OMPS, TROPOMI), N. Loeb (Radiation Field), V. Realmuto (IR), M. L. Santee (Chem), J-P. Vernier, J. Welton (Lidar), S. Carn, F. Schwandner (OCO-2 & OCO-3)

6.1. Introduction

Unlike suborbital measurement capabilities, satellite instruments that could be used to characterize and monitor volcanic clouds are either operating in advance of the eruption or coincidentally very soon after, as it is unlikely that a satellite mission could be developed from scratch and deployed in time to contribute. As such, we can be fairly certain of the maximal set of existing and planned satellite resources to be considered here, as is summarized in Table 8.

The satellite contribution to the near-term response, and to longer-term study, of a major volcanic eruption is frequent, globally-extensive coverage. In addition to monitoring the injection and 3-D spatial distribution of emitted gases, ash, and sulfate plumes, satellites can put limits on the amount of aerosol and gases, and to some extent determine the aerosol type. Satellite global-scale mapping, of value in itself, can be used to constrain and validate models, allowing for gap-filling where measurements are lacking, and to some extent, prediction of future climate, chemistry, and broad environmental impacts. Space-based Interferometric Synthetic-Aperture Radar (InSAR) missions can also detect cm-scale surface deformations that might signal possible eruptions from even long-dormant volcanoes.

Table 8. Currently operational (March 2018) and near-future satellite missions with volcanic plume/thermal monitoring capabilities

Satellite	Sensors	Launch date	Volcanic features monitored[1]	Overpass time (local)[2]	Resolution		Websites[5]
					Spatial[3]	Temporal[4]	
Low Earth Orbiting (LEO)							
NOAA-15	AVHRR/3 HIRS/3	13 May 1998	Hot-spots, ash UTLS SO_2	7:30 am	1 km 18 km	Daily Daily	USGS: http://volcview.wr.usgs.gov/
Landsat 7	ETM+	15 Apr 1999	Hot-spots	9:45 am	15-60 m	16 days	Landsat Science: http://landsat.gsfc.nasa.gov/
NASA Terra	MODIS ASTER MISR CERES MOPITT	18 Dec 1999	Hot-spots, SO_2, ash, AOD Hot-spots, SO_2, ash, aerosols Ash/Sulfate AOD, near-source plume height TOA and surface radiation budget CO	10:30 am	250 m – 1 km 15-90 m 275m -1 km 20 km 22 km	2× daily 16 days ≤ 9 days 1 day	MODVOLC: http://modis.higp.hawaii.edu/ ASTERWEB: http://asterweb.jpl.nasa.gov AVA: http://ava.jpl.nasa.gov/ MISR at JPL: http://www-misr.jpl.nasa.gov/ NCAR: https://www2.acd.ucar.edu/mopitt
COSMO-SkyMed	4 satellite constella-tion, X-band SAR	8 June 2007 9 Dec 2007 25 Oct 2008 5 Nov 2010	Ground deformation	06:00 (90° phasing btwn satellites)	3 m (HIMAGE Stripmap Mode)	16 days	ASI: http://www.cosmo-skymed.it/en/index.htm
Sentinel-1A	C-band SAR	3 Apr 2014	Ground deformation	06:00	5 m (Strip Map Mode)	12 days	ESA: https://earth.esa.int/web/guest/missions/esa-operational-eo-missions/sentinel-1
Sentinel-1B	C-band SAR	25 Apr 2016	Ground deformation	06:00	5 m (Strip Map Mode)	12 days	ESA: https://earth.esa.int/web/guest/missions/esa-operational-eo-missions/sentinel-1
ALOS-2	PALSAR-2 (L-band SAR)	24 May 2014	Ground deformation	12:00 (descending orbit)	10 m (Stripmap Mode)	14 days	EORC/JAXA: http://www.eorc.jaxa.jp/ALOS/en/
NISAR	L-band SAR	TBL: 2021	Ground deformation	TBD	12 x 8 m (Background Land Mode)	12 days	http://nisar.jpl.nasa.gov/
NASA EO-1	ALI Hyperion	21 Nov 2000	Hot-spots Hot-spots	10:00 am	10-30 m 30 m	16 days 16 days	USGS: http://eo1.usgs.gov/

Odin	OSIRIS	20 Feb 2001	750 nm extinction profiles, AOD	6:00pm sunlit: NH May-Aug; SH Nov-Feb	2(v) km; 5 deg (~550 km) along-track spacing	Daily near-global	http://osirus.usask.ca/?q=node/293
NASA Aqua	MODIS AIRS CERES	4 May 2002	Hot-spots, SO_2, ash, AOD UTLS SO_2, ash, aerosols TOA and surface radiation budget	1:30 pm	250 m – 1 km 13.5 km 20 km	2× daily 2 days 1 day	MODVOLC: http://modis.higp.hawaii.edu/ SACS: http://sacs.aeronomie.be/nrt/
CSA SCISAT	ACE-FTS	Feb 2004 (Launch Aug 2003)	SO_2, HCl, sulfate aerosols	varies	3-4(v)×4× 500(h) km footprint	Solar occultation	http://www.ace.uwaterloo.ca/data.html (current dataset available only to ACE Science Team members)
NASA Aura	OMI	15 Jul 2004	SO_2, BrO, OClO, ash	1:45 pm	13×24 km	~Daily	NASA: http://so2.gsfc.nasa.gov/
NASA Aura	MLS	15 Jul 2004	UTLS SO_2, H_2O, HCl, CH_3Cl	1:45 pm	3-4(v) ×6× 200-500(h) km footprint; 165 km along-track spacing	Twice daily near-global	http://mirador.gsfc.nasa.gov/cgi-bin/mirador/homepageAlt.pl?keyword=MLS
NOAA-18	AVHRR/3 HIRS/4	20 May 2005	Hot-spots, ash UTLS SO_2	1:30-2:30 pm	1 km 10 km	Daily Daily	USGS: http://volcview.wr.usgs.gov/
NASA: ISS	SAGE-III	2017	Vertical profiles ~10km-80km: O_3, SO_2, NO_2, ash, aerosols				
NASA-ISS	ECOSTRESS	TBL: 2018	Hot spots, SO_2, ash	variable	40 x 70 m	2 – 3x daily	http://ecostress.jpl.nasa.gov/
ESA: Earth Care	ATLID	TBL: 2018	Profiles and layer averaged products: depolarization, extinction, backscatter at 355nm		? (vert) ? (horizont)		
NASA/CNES CALIPSO	CALIOP	28 Apr 2006	Profiles and layer averaged products: depolarization, extinction, backscatter, 532nm, 1024nm	1:31 pm	333 m (horiz.)	16 days	http://www-calipso.larc.nasa.gov/
CloudSat	CPR	28 Apr 2006	Hydrometeors, ash aggregates	1:31 pm	~1.5 km	16 days	http://cloudsat.atmos.colostate.edu/
EUMETSAT MetOp-A	GOME-2 IASI	19 Oct 2006	SO_2, BrO, OClO, ash SO_2, H_2S, CO, ash, aerosols	9:30 am	80×40 km 12 km	~Daily 2× daily	SACS: http://sacs.aeronomie.be/nrt/ http://cpm-ws4.ulb.ac.be/Alerts/index.php

	AVHRR/3 HIRS/4		Hot-spots, ash UTLS SO$_2$		1 km 10 km	Daily Daily	http://www.nsof.class.noaa.gov/
NOAA-19	AVHRR/3 HIRS/4	6 Feb 2009	Hot-spots, ash UTLS SO$_2$	1:30-2:30 pm	1 km 10 km	Daily Daily	USGS: http://volcview.wr.usgs.gov/
NASA/NOAA Suomi NPP	OMPS VIIRS CrIS	28 Oct 2011	SO$_2$, ash Hot-spots, SO$_2$, ash UTLS SO$_2$, ash, aerosols	1:30 pm	50 km 375-750 m 14 km	Daily 2× Daily Daily	NASA: http://so2.gsfc.nasa.gov/ http://viirsland.gsfc.nasa.gov/index.html http://npp.gsfc.nasa.gov/cris.html
NASA Suomi NPP, JPSS-2	OMPS – Limb Profiler	28 Oct 2011	Vertical profiles ~10 km-80 km: O$_3$, SO$_2$, ash, aerosols	1:30 pm	2 km (vertical), sampling 1 km, 280-1000 nm ? (horizontal)	Daily	NASA: http://ozoneaq.gsfc.nasa.gov/omps extinction detection limit ~0.0001 km-1
EUMETSAT MetOp-B	GOME-2 IASI AVHRR/3 HIRS/4	17 Sep 2012	SO$_2$, BrO, OClO, ash SO$_2$, H$_2$S, CO, ash, aerosols Hot-spots, ash UTLS SO$_2$	9:30 am	80×40 km 12 km 1 km 10 km	~Daily 2× daily Daily Daily	SACS: http://sacs.aeronomie.be/nrt/ http://cpm-ws4.ulb.ac.be/Alerts/index.php http://www.nsof.class.noaa.gov/
Landsat 8	OLI, TIRS	11 Feb 2013	Hot-spots, ash	10:00 am	15-100 m	16 days	USGS: http://landsat.usgs.gov/landsat8.php
NASA OCO-2	OCO-2	2 Jul 2014	CO$_2$	1:15 pm	1.3×2.3 km	16 days	http://oco.jpl.nasa.gov/
ESA Sentinel-2	MSI	2014	Hot-spots	10:30 am	10-60 m	5 days	
ESA Sentinel-5 Precursor	TROPOMI	2016	SO$_2$, BrO, OClO, ash	1:35 pm	7×7 km	Daily	http://www.tropomi.eu/TROPOMI/Home.html
			Geostationary (GEO)				
EUMETSAT Meteosat-7	MVIRI	9 Feb 1997	Hot-spots	n/a	2.5-5 km; 57ºE	30 min	
CMA FY-2E	S-VISSR	19 Oct 2004	Hot-spots, ash	n/a	1.25-5 km; 105ºE	30 min	http://www.ssec.wisc.edu/data/geo/
EUMETSAT Meteosat-9	SEVIRI	22 Dec 2005	Hot-spots, ash, SO$_2$	n/a	1-3 km; 9.5ºE	5 min	http://volcano.ssec.wisc.edu/ http://fred.nilu.no/sat/
JMA MTSAT-2	Himawari-7	18 Feb 2006	Hot-spots, ash	n/a	1.25-5 km; 145ºE	30 min	http://volcano.ssec.wisc.edu/
CMA FY-2D	S-VISSR	15 Nov 2006	Hot-spots, ash	n/a	1.25-5 km; 87ºE	30 min	http://www.ssec.wisc.edu/data/geo/

GOES-14 (E)	Imager	27 Jun 2009	Hot-spots, ash	n/a	1-4 km; 75ºW	1 min	http://volcano.ssec.wisc.edu/
GOES-15 (W)	Imager	4 Mar 2010	Hot-spots, ash	n/a	1-4 km; 135ºW	1 min	http://volcano.ssec.wisc.edu/
KMA COMS-1	MI	26 Jun 2010	Hot-spots, ash	n/a	1-4 km; 128ºE	10 min	http://www.ssec.wisc.edu/data/geo/
CMA FY-2F	S-VISSR	13 Jan 2012	Hot-spots, ash	n/a	1.25-5 km; 113ºE	30 min	
EUMETSAT Meteosat-10	SEVIRI	5 Jul 2012	Hot-spots, ash, SO_2	n/a	1-3 km; 0º	15 min	http://volcano.ssec.wisc.edu/ http://fred.nilu.no/sat/
JMA MTSAT	Himawari-8	2014	Hot-spots, ash, SO_2	n/a	0.5-2 km; 145ºE	2.5 min	http://mscweb.kishou.go.jp/himawari89/
GOES-R	ABI	Early 2016	Hot-spots, ash, SO_2	n/a	0.5-2 km; 75º/137ºW	30 sec	http://www.goes-r.gov/
L1 Lagrange libration point							
NOAA DSCOVR	EPIC	2014-15	SO_2, ash	n/a	8 km; sunlit Earth disk	90 min	http://www.osd.noaa.gov/DSCOVR/dscovr.html

6.2. Near term plan (0-1 month after the eruption)

6.2.1. One-Day Response

The satellite response within a day of the eruption would include:

- **≤ 1 hour:** First observations of **volcanic plume extent and dispersion.** Some constraints on **height** will come from geostationary imagers covering spectral channels from the visible to the thermal IR.
- **1-6 hours: Maps of the horizontal extent of ash and/or SO$_2$ clouds** will be available from operational TIR mappers with +3 hour near-real-time data processing latency, day or night. Automatic alerts will be generated by operational agencies, such as European Support to Aviation Control Service (SACS) and the global network of Volcanic Ash Advisory Centers (VAAC's), along with their best estimates of plume 3-D extent and dispersion. High-resolution images will be available from direct broadcast MODIS and VIIRS imagers.
- **≤ 1 day: Maps of volcanic SO$_2$ and ash clouds** will be available from polar UV and vis-NIR mappers that rely on backscattered solar illumination. NOAA will generate automatic alerts based on UV and TIR data. Also, initial lower-limit estimates of the **total injected SO$_2$ mass, and the height** of the center of mass of the SO$_2$ plume will be acquired by UV and TIR mappers.
- **~ 1 day:** Depending on plume opacity and location relative to instrument sampling, passive limb-viewing instruments (e.g., OMPS-limb profiler, MLS, SAGE), narrow-swath, multi-angle imagers (e.g., MISR), wide-swath, cross-track imagers (AVHRR, MODIS, VIIRS), wide-swath broadband radiometers (CERES) and active-sensor lidar might provide **aerosol layer heights or profiles**, some constraints on **aerosol type** and **SO$_2$ profiles**.

Links to volcanic cloud alerts, UV, VIS, and IR SO$_2$ maps with tonnage calculations will be provided at the NASA volcanic SO$_2$ web site[1].

6.2.2. One-Week Response

Within a week or two, as SO$_2$ begins to convert to sulfate aerosol, aerosol and gas clouds are spread widely by prevailing winds. Satellites will acquire more volcanic cloud observations, and lidars will likely provide at least some aerosol vertical profiles together with information on ash and sulfate using depolarization measurements. VIS-NIR mappers will map enhanced column aerosol optical thickness. Multi-angle imagers will provide some aerosol size, shape and height information, depending on aerosol distribution and optical depth, and microwave limb and solar occultation sounders will provide profiles of SO$_2$ and other emitted gases, such as water vapor and HCl. Broadband radiometers will provide first estimates of the top-of-atmosphere radiative effect of the event. One of the CERES instruments could be commanded to optimize its scan pattern to "dwell" on the area affected by the volcanic eruption. Large-swath imagers will likely have acquired the plume multiple times, making initial aerosol cloud evolution and dispersion studies possible, estimating SO$_2$ decay rate and allowing for improved modeling of cloud behavior.

---

[1] http://so2.gsfc.nasa.gov

Satellite data combined with back-trajectory analysis can provide initial estimates of volcanic emission source strength and SO_2-cloud center-of-mass elevation. For very large eruptions, UV/vis limb-viewing sensors (e.g., SAGE and OMPS-limb profiler) are unlikely to be able to probe below the top of the thick aerosol layer, whereas instruments measuring microwave emission will continue to probe deeper into the atmosphere.

6.3.   Long term plan (>1 month after the eruption)

As the volcanic perturbation evolves and the length of the available satellite data-record increases, more detailed studies become possible. Volcanic cloud evolution and dispersion studies, integrating multiple space- and surface-based measurements into models can then be pursued. In particular, the physical and chemical evolution of the cloud can be characterized, based on the aggregate of observations, including targeted, localized measurements from aircraft and/or balloon-borne instruments that offer validation data and detail unobtainable from remote sensing. Satellite mapping will also contribute to targeting decisions for the suborbital platforms. Aerosol and gas source strengths and loss mechanisms can also be derived from modeling constrained by the aggregate of these data.

The data collected (from eruption onset through the ensuing months and years, as conditions return to the background state) will provide critical tests of global climate models, and refined estimates of the volcano's impact. The chemistry-climate community will want to assess whether the models correctly represent the time-evolution of perturbations to Earth's energy budget from the top-of-atmosphere to the surface, the hydrological cycle, ocean heat uptake and sea level rise, atmosphere and ocean dynamics, and the global mean and regional temperature responses. With a comprehensive suite of observations, models can be strengthened and limitations found.

Chemistry-climate models, constrained by the aggregate of observations, will be used to update impact predictions on surface temperatures, precipitation, ozone, and diffused sunlight on seasonal and longer timescales. The constrained model results could provide crucial additional information needed to mitigate the agricultural consequences of a large eruption, for example, by adapting crops to expected changes in temperature and humidity.

7.   Ground-based observations

Ellsworth J. Welton, Paul Stackhouse

7.1. Introduction

Obtaining information on volcanic emissions from surface measurements on short times scales will require some serendipity, since the large majority of these sites are fixed and rely upon the plume aerosols and gases to flow overhead. Additionally, almost all of these sites require cloud free periods during the day for observation. A notable example is the recent short volcanic eruption of Bogoslov (May 27, 2017), where the emissions were limited to one explosive eruption to the atmosphere and exceedingly cloudy conditions hindered rapid characterization. Next to fixed sites, there are also mobile, deployable networks. These, however, would require a few weeks to be deployed at locations where they could observe the volcanic plume.

While some ground network sites have near-real time capabilities, others require time for the site investigator to download, process and access the measurements. Depending upon the network and complexity, the provision of the data products varies from a few days to over a year.

Ground network can provide various measurements for the characterization of volcanic plumes (Table 9). Perhaps, the most useful are active surface measurements, such as lidar networks (Section 7.2.2) that provide profile information about aerosols. The next class of measurements are passive measurements of solar radiation that measure that transmittance of solar irradiance to the surface either for broadband, selected wavelengths or high resolution spectra (Section 7.2.1). These measurements are used in algorithms to retrieve information about the total aerosol and/or total gaseous constituents of the atmosphere. Finally, there are a number of atmospheric composition instruments deployed

Table 9: Generalized classes of surface measurements that would provide information relevant to volcanic aerosol and gaseous emissions

Class	Vertical Extent	Temporal Extent	Observing Conditions	Example Data Products
Active profiling	Up to 30 km	24 hours	Thin clouds	AOD, single scattering albedo, size distribution, particle shape, aerosol/cloud height, PBL structure
Passive solar broadband irradiance (pyrheliometer, radiometer)	Whole atmospheric transmission	Daytime only	Clear	Solar total irradiance, direct normal radiation, diffuse fluxes, transmittance
Passive solar spectral radiance (CIMEL, MFRSR, Pandora, etc.)	Whole atmospheric transmission	Daytime only	Clear	Spectral transmission, Angstrom coefficient, coarse mode AOD, total gases, O_3, NO_2, SO_2
***In-situ* meteorological and gaseous measurements**	Up to 10 m	Up to 24 hours	All-sky	Temperature, humidity, winds, precipitation, aerosol constituents and mass; gaseous pollutants, SO_2, O_3, CO, PM2.5

at stations around the globe that would have direct impacts on the understanding of a volcanic cloud.

7.2. Instrument assets

7.2.1. Surface Radiation and Aerosol Measurements Networks

High quality surface radiative measurements are made at relatively few places around the world. The world standard for the measurements of broadband solar irradiance is maintained by the GEWEX/GCOS (Global Energy and Water Cycle Exchange Program/Global Climate Observing System) Baseline Surface Radiation network (BSRN[2]). A global distributed map of BSRN sites is shown in Figure 3. Each BSRN site manager maintains, calibrates, processes and delivers measurements from shaded and unshaded pyranometers and active cavity radiometers. The shaded pyranometer and the Normal Incident Pyrheliometer (NIP) provide an estimate of the diffuse and direct normal broadband solar components. The unshaded pyranometer measurements are used for comparisons. Other measurements made at the site are required for validation or are augmented by the site management. For instance, the NOAA SURFRAD network, which meets BSRN standards and archives data at the central archive, also provides measurements using an UV-A, UB-B, PAR and MFRSR instrument, from which aerosol optical depth and other variables are retrieved.
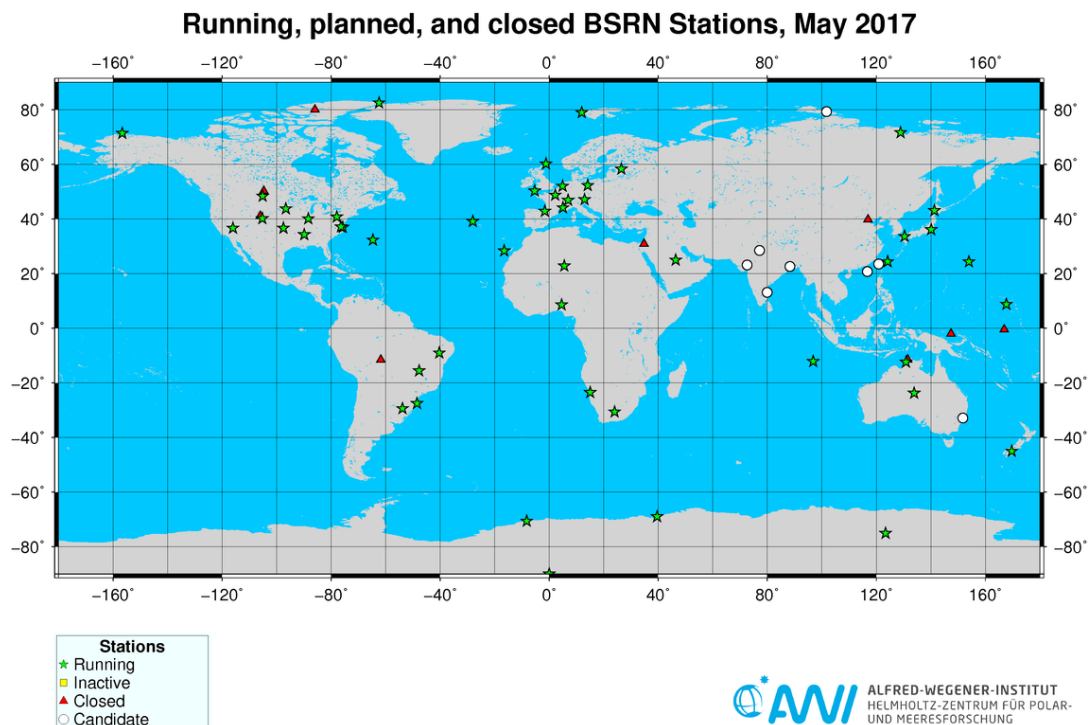

Figure 3: Map of BSRN sites that provide surface measurements of radiative quantities including direct normal irradiance.

_____

[2] http://bsrn.awi.de/

Measurements from the BSRN network are typically archived well after they are taken, but no later than two years, as requested by BSRN standards. Certain site managers may be able to make initial data products available sooner. For instance, the NOAA SURFRAD network provides data sets via their web site within a couple days.

A well-established ground network of aerosol measuring sites is the AErosol RObotic NETwork (AERONET[3]). AERONET provides a long-term continuous database of aerosol optical, microphysical and radiative properties provided by instruments following a standardized calibration, processing, and distribution. AERONET provides near-global coverage spectral AOD (Figure 4), and data are generally available within an hour. While AERONET has been mainly used for total column AOD, Ridley et al. (2014) showed that stratospheric AOD can be derived from AERONET data even in non-volcanic conditions from a selection of sites distributed between 28°S and 80°N.
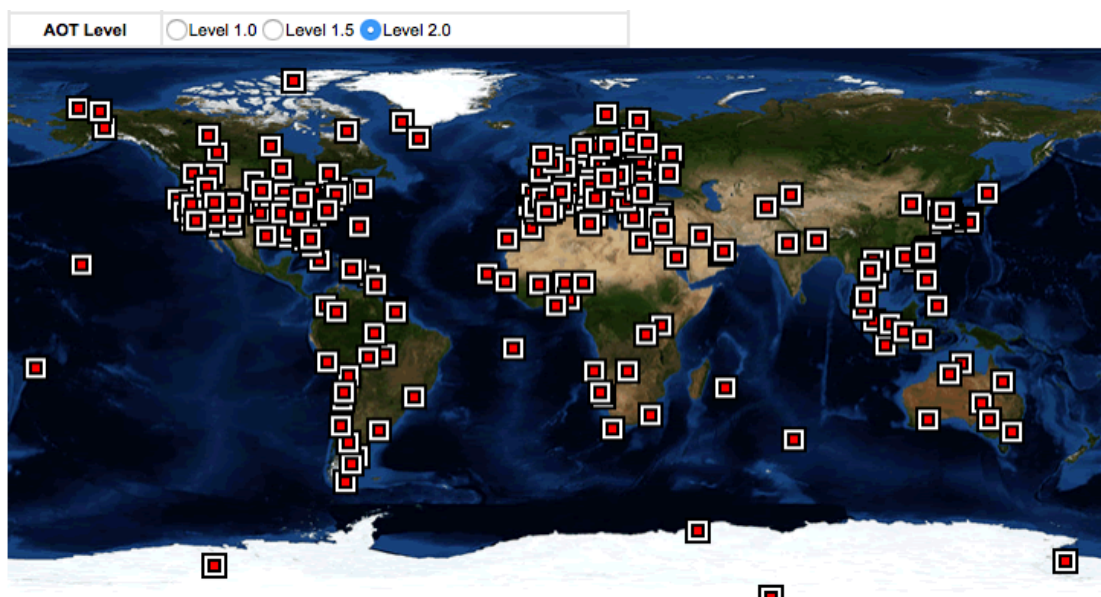

Figure 4: Map of AERONET sites providing Level 2.0 data for the year 2016.

7.2.2. Lidar Networks

The NASA Micro-Pulse Lidar Network (MPLNET[4]) is a global federated network of polarized Micro-Pulse Lidar (MPL) systems designed to measure aerosol and cloud vertical structure continuously, day and night, over long time periods. MPLNET currently includes 17 long-term and numerous short-term field campaign sites. There are 6 more sites in planning stages towards operational status by end of 2017 and several more at proposal stage. Most MPLNET sites are co-located with sites in the NASA Aerosol Robotic Network (AERONET). These joint super sites provide both column and vertically resolved aerosol and cloud data, such as: optical depth, single scatter albedo, size distribution,

---

[3] https://aeronet.gsfc.nasa.gov

[4] http://mplnet.gsfc.nasa.gov

fine/coarse mode, aerosol and cloud heights, particle shape, planetary boundary layer (PBL) structure and evolution, profiles of aerosol and thin cloud extinction and backscatter, and continuous day/night column and PBL aerosol optical depth.

MPLNET utilizes small, low-powered, eye-safe lidars that provide data continuously offering comprehensive diurnal coverage. Appendix A1 provides a detailed summary of the ability of MPLNET to detect volcanic plume layers. In summary, MPLNET would have no problem detecting volcanic eruptions of the order this report focuses on (VEI +4). This capability will extend for several years after the eruption, after which the low signal-to-noise ratio of MPLNET will not allow the detection of the volcanic aerosol.

MPLNET is a member of the WMO Global Atmospheric Watch (GAW) Aerosol Lidar Observation Network (GALION, Figure 5), which currently includes: MPLNET (NASA), EARLINET (EU), AD-NET (Japan), NDACC (lidar component), LALINET (South America), and CREST (NOAA).
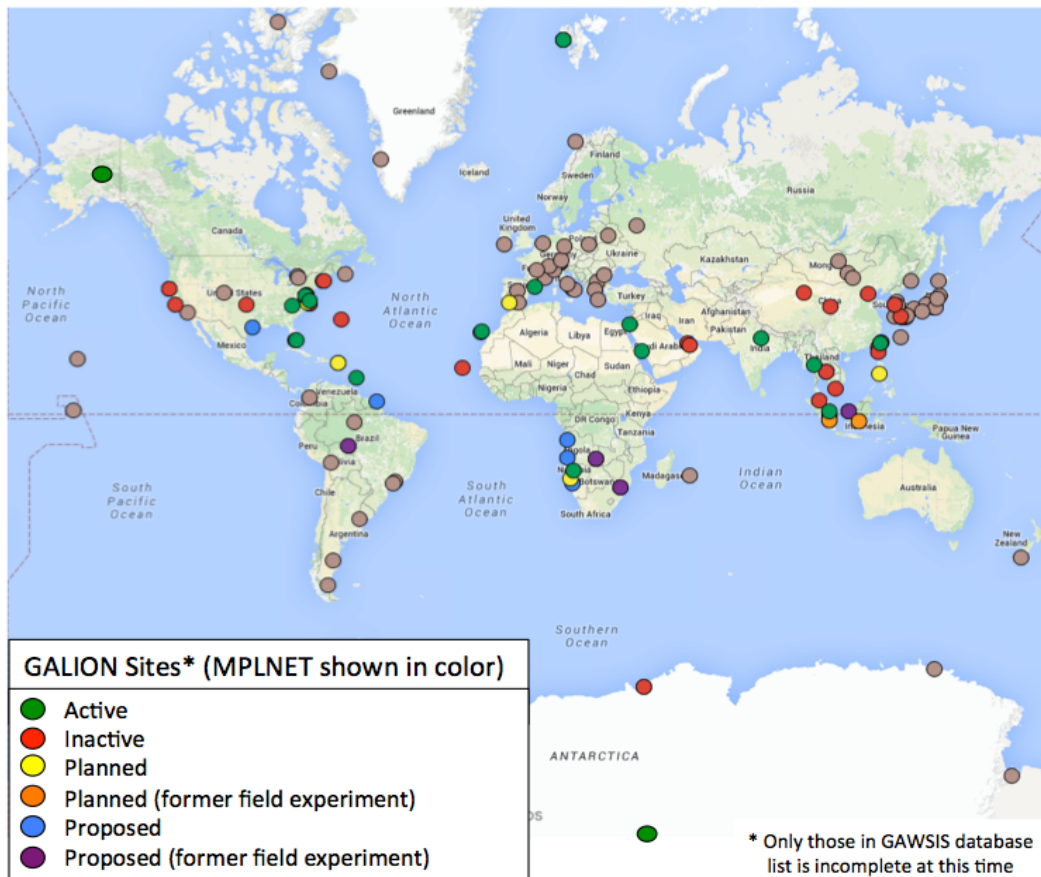

Figure 5 Map of GALION sites that have been entered into the WMO GAWSIS database system. This is not a comprehensive list of all GALION sites and efforts are ongoing to complete the GAWSIS entries as well as begin development of a GALION data center.

7.2.3. Atmospheric Composition Ground Networks

Ground based ozone observations are based on the Brewer-Dobson global set of total ozone observation stations and on observations by the Network for the Detection of Atmospheric Composition Change (NDACC [5]) from UV-Vis DOAS, microwave instruments, and Fourier transform infrared observations (FTIR). In addition to these networks, NASA has some deployable capabilities with respect to Pandora spectrometers (UV-vis observations 280-525 nm).

The Brewer-Dobson network of total ozone observations is global, and the data collection is centered at the World Ozone and Ultraviolet Radiation Data Centre (WOUDC [6]). WOUDC is a WMO data center operated by Environment and Climate Change Canada in support of the Global Atmosphere Watch (GAW) program. There are over 450 stations listed in the WOUDC records, of which approximately 123 reported total ozone observations in 2014. These instruments would be the prime ground evaluation of the effects on total ozone column of a passing volcanic cloud. A contact listing of these sites should be implemented by NASA for notifying operators of the imminent approach of a volcanic cloud. In principle, the Brewer instruments can also be used to make quantitative estimates of volcanic total column SO_2.

The NDACC network (Figure 6) is composed of more than 70 high-quality, remote-sensing research stations for observing and understanding the physical and chemical state of the stratosphere and upper troposphere. The NDACC stations have both lidars and ground instruments that are extremely useful for observing volcanic clouds. In particular, observations of ozone, H_2O, NO_2, and halogenated species are directly relevant to a volcanic cloud's initial structure and evolution. As noted in

Table 3, observations of HCl are key to understanding how a major eruption would impact the stratosphere, and this gas is directly measured by the FTIR instruments. Further, concentrations of NO_2 are perturbed by heterogeneous reactions on the surface of volcanic sulfate aerosol particles, and these NO_2 perturbations can be observed by the NDACC UV-vis spectrometers (more than 30 deployed around the globe).

Similar to NDACC, the Total Carbon Column Observing Network network features > 25 operational high-quality remote sensing research stations for physical and chemical characterization of the atmosphere, routinely used for satellite validation (e.g., GOSAT, OCO-2). Their high-resolution sun-tracking Fourier Transform Spectrometers record direct solar spectra in the near-infrared spectral region. From these spectra, accurate and precise column-averaged abundance of CO_2, CH_4, N_2O, HF, CO, H_2O, and HDO are retrieved.

The Pandora spectrometers are both portable and inexpensive. Pandora instruments provide observations of O_3, NO_2, and potentially SO_2. Pandora instruments could be rapidly deployed to remote sites to provide and support ground estimates of plume motion, ozone and NO_2 changes, and SO_2 conversion to sulfate aerosol. Future plans of the Pandora Project include the near-real-time to real-time processing and dissemination of the data via the internet.
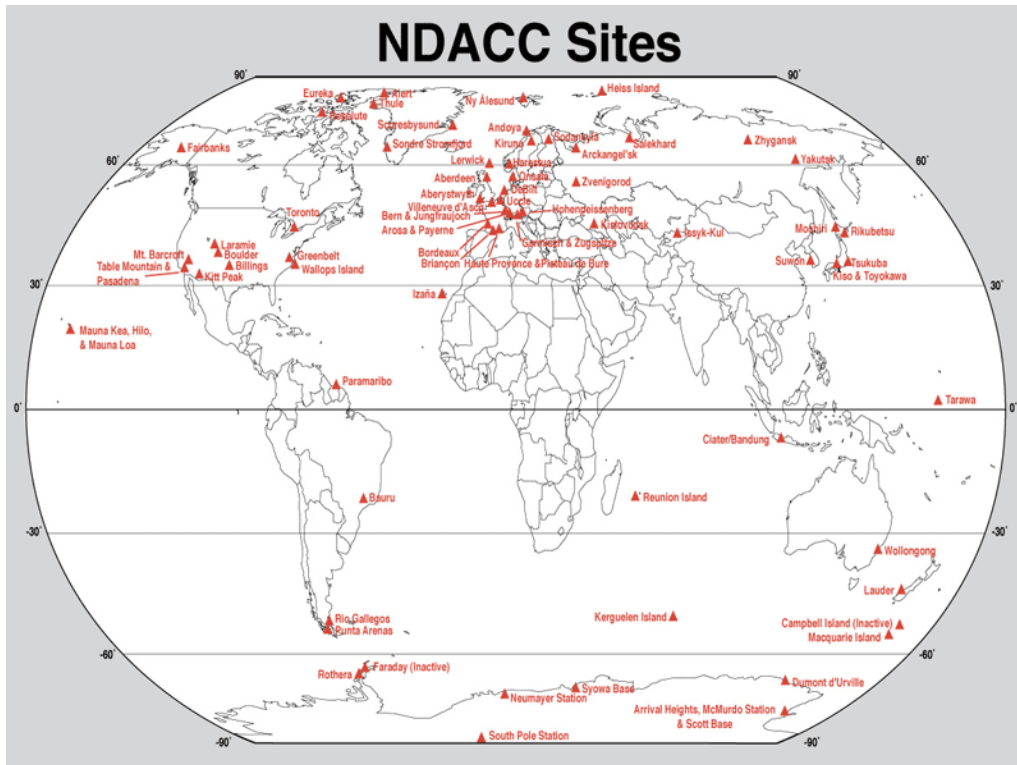
---

[5] http://www.ndsc.ncep.noaa.gov/

[6] http://woudc.org/

Figure 6: Map of NDACC sites

7.3. Preparatory Actions

Of the networks described in the sections above, only NDACC was created to monitor the stratosphere. Within the other networks (GALION, MPLNET, and AERONET) only some instruments have the capability to profile the stratosphere and pre-existing, automated, and quality tested stratospheric data products are not readily available. In this respect, MPLNET and GALION partners are already planning actions that would overcome many existing deficiencies to support stratospheric volcano plume observations:

1. The GALION steering committee and GAW leadership have agreed to develop a GALION specific data center to provide a consolidated access point for lidar network information and data. This effort was planned and initiated at the 2017 GALION meeting (June 25-30, 2017). The GALION data center will provide comprehensive discovery tools to show locations of all lidar sites, including filtering by capability such as ash-sulfate discrimination, size resolution, and optical depth. This will allow improved deployment planning in the event of an eruption. The GALION data center will also provide a streamlined data download capability across GALION networks.

2. At the upcoming GALION meeting (2016) it will be proposed to institute a formal volcano working group be established. An ad-hoc group exists already, but with focus on tropospheric eruptions. The GALION volcano working group would be charged with developing stratospheric lidar products, first within their respective

networks and then with a common GALION product suite. The group would also formulate an eruption response plan to alert GALION members and help coordinate activities.

3. MPLNET will begin development of a stratospheric aerosol product in 2017. MPLNET level 1 data extend from the surface to 30 km asl. Thus, MPLNET has the technical capability to profile much of the stratosphere.

7.4. Near term plan (0-1 month after the eruption)

Being already operative at the time of the eruptions, if located in a favorable position ground networks can provide measurements from a very early stage of the volcanic plume development. AERONET will provide column aerosol optical thickness, providing data on the formation and transport of the volcanic aerosol. MPLNET will provide continuous (24/7) data on plume height, and ash vs. sulfate discrimination. GALION stations will provide: determination of volcanic plume height and discrimination of plume ash vs. sulfate from polarized lidar stations. Estimation of aerosol size and composition will be provided from advanced lidar stations. These data products will be available from the AERONET and MPLNET data center websites in near real time (NRT, < 2 hours). The same data, and enhanced volcanic specific products will be available from the GALION data center after its activation. All stations will be alerted to a major eruption and asked (where appropriate) to provide early reports on the volcanic cloud appearance over the station.

MPLNET and several GALION members are already working to provide routine, automated NRT data products to operational aerosol forecasting centers (e.g. ICAP) and VAAC operations. These activities will continue and should be considered part of the responses detailed here.

7.4.1. One-Day Response

The ground network response within a day of the eruption should be considered a potential response due to dependence on the location of the eruption relative to existing lidar stations. The response detailed here only applies to those sites under the plume path on day one.

1. **0 - 3 hours:** Initial plume data would be available from sites with NRT data capability.
2. **3 - 24 hours:** Additional plume data will become available from sites without NRT capability. Alerts will be issued across networks to inspect current data and verify that instruments are active and working properly. Special attention will be paid to those most likely to be in immediate advection path of the plume. It is expected that during this time GALION volcanic working group team members will be interacting with VAAC members in areas affected by the eruption and providing similar alerts to monitor potential impacts to navigation and human health.
3. **1 day:** A station report will be compiled. The report will include a list of the operational and non-functional sites, with summary of the problems, estimated time till operational, and estimates of any repair costs needed to reach operational status. If the eruption is major, a global station alert will be broadcast, with a projection of plume movement (as forecast from model simulations).

7.4.2. One-week Response

Stations would continue to provide plume data. Stations near the plume would be alerted, and emphasis will be placed on assisting those non-functional lidar stations in the path of the plume. MPLNET will begin repair of any non-functional critical sites.

MPLNET will determine if any lidars are available for rapid deployment to critical observation sites lacking current lidar coverage.

The GALION volcanic working group will assemble all collected data and begin preparing summary data products (Level 3), plots, and report material.

7.5. Long term plan (>1 month after the eruption)

Stations would continue to provide plume data. Report actions will shift from repair of non-functional sites to assessment of operational sites, with estimates of long-term health outlook of the instruments and anticipated down-time (such as known subcomponent failures, diode or flash lamp supply). A plan will be drafted to maintain critical lidar sites.

8. Aircraft-observations observations

8.1. Introduction

Aircraft can provide detailed sampling over broad areas with comprehensive and synergistic payloads that can detail information needed for the characterization of the volcanic plume. Aircraft partner with satellites (providing global, daily coverage), balloons (probing to high altitudes > 30 km), and ground observations (24/7 high temporal resolution) to provide a complete picture of the volcanic aerosol.

Heavy lift aircraft (e.g., NASA's DC-8, G-V) can provide in-situ observations up to 12 km (only into the lowest part of the stratosphere). Figure 7 shows simulated zonal mean equatorial SO_2 from the Mt. Pinatubo eruption. As is clear, the mass of the plume is located above the maximum altitude range of the NASA DC-8 (~12 km). However, a payload of remote sensing instruments (including upward looking lidars) could easily map this plume to high altitude.
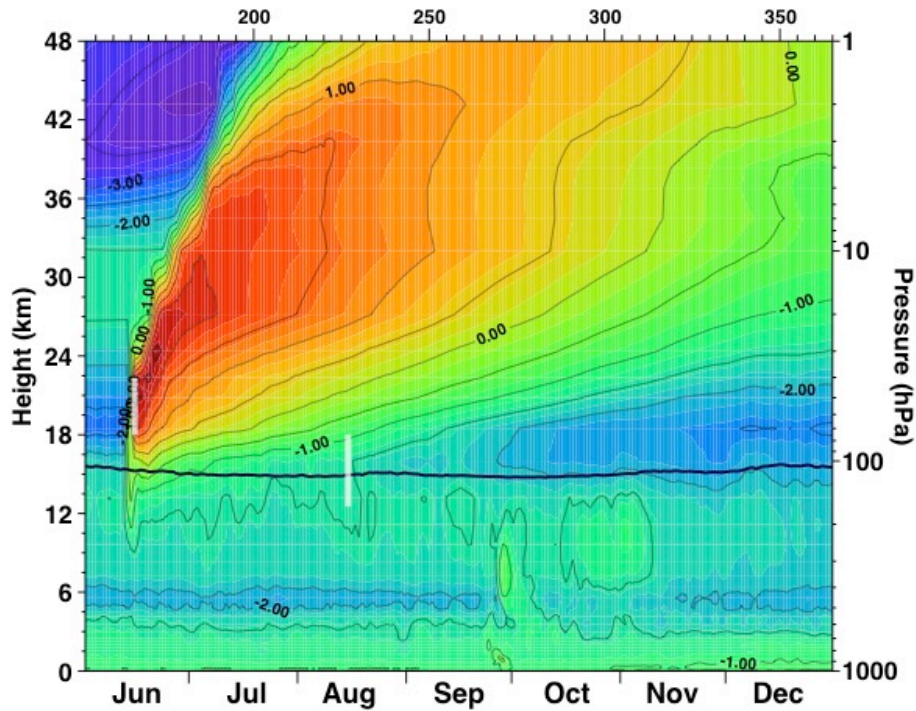
Figure 7: Time versus altitude plot of simulated SO₂ concentrations following an eruption of Mt. Pinatubo in June, and Cerro Hudson in August (marked by white lines). Concentrations are plotted on a log scale, where the value 1 represents 10 ppbv of SO₂. The GEOSCCM model output is a zonal mean meridional 0-20˚N average.

High altitude aircraft (e.g., NASA's ER-2, WB-57f, and Global Hawk) can make in-situ observations of stratospheric volcanic clouds. The ability to carry a heavy payload to altitudes greater than 18 km is key to obtaining the in-situ observations outlined in Table 2 and

Table 3. For example, in Figure 7, a model simulation of equatorial SO₂ is elevated over the background of 0.01 ppbv at 18 km for 3 months following the eruption.

This section is organized in four parts. The first section discusses the necessary payloads, the second outlines the available NASA aircraft platforms, the third discusses the deployment timeline, and the final section outlines potential deployment sites.

8.2. Payloads

The payloads for the aircraft depend on the specific period that follows the eruption. The specifics of the aircraft deployment timeline are shown in a subsequent section. For planning purposes, we assume that the top-priority instruments are those that: 1) make critical observations (see Table 2 and

Table 3), and 2) can be rapidly integrated onto the NASA aircraft (see platforms below). In developing this plan, we assume that one of our aircraft is for high-altitude sampling in the stratosphere and the second is a heavy-lift tropospheric aircraft with a continental-scale sampling range.

The high-altitude stratospheric sampling platform is essential during the early period after the eruption, but might not be necessary later on. As is clear from Figure 7, a

high-altitude aircraft ($z > 18$ km) can observe SO_2 concentrations greater than 10 ppt only for about 3 months following an eruption. Hence, the high-altitude payload will depend on the time-scale with which the aircraft can be deployed. NASA has flown numerous instruments in the stratosphere over the last few decades. In fact, the NASA U-2 was flown into the Mt. St. Helens plume 24 hours following the eruption.

The high-altitude payload is derived from previously flown high-altitude instruments to measure injected compounds, aerosols, and primary stratospheric trace species (see Table 12), rather than reactive species. A total of 9 instruments are prioritized in the table, with two overlapping remote sensing instruments that will be down-selected to a single instrument depending on deployment readiness. Because the volcanic plume will be concentrated in the free stratosphere, the heavy-lift tropospheric payload focuses on remote sensing instruments. Table 11 displays four prioritized instruments that are focused on volcanic particles, injected species, and NO_2.

The payloads outlined above are specifically tailored to the initial deployments that occur within a few months of the eruption. Subsequent deployments would require additional instruments and capabilities that would be focused on the evolution of the plume and stratosphere.

8.3. Aircraft Platforms

NASA has an exceptional suite of aircraft that can be deployed to examine a major volcanic eruption. The NASA Airborne Science Program (ASP) not only owns and operates aircraft, but also has a number of partnership arrangements with other government agencies and private contract aircraft[7]. The NASA aircraft that are under immediate control could be quickly tasked for a volcanic plume sampling campaign. Table 10 shows the principal NASA aircraft that could be deployed along with their principal operational characteristics. The aircraft in this table are partitioned into aircraft that primarily sample in the lowest-most stratosphere or troposphere, and the free stratosphere (> 50 kft).

---

[7] https://airbornescience.nasa.gov

Table 10: NASA Airborne Science Program Aircraft

NASA ASP platform	Center	Duration (hr)	Payload (tons)	GTOW (tons)	Max Alt (kft)	Air Spd (kts)	Range (kNmi)
Heavy lift tropospheric							
C-130H (a)	WFF	10	18.0	78	23	320	3.2
P-3 Orion (b)	WFF	14	7.4	68	32	400	3.8
DC-8 (c)	AFRC	12	15.0	170	41	450	5.4
G-III (C-20A) (d)	AFRC	7	1.3	35	45	460	3.4
G-III (e)	JSC	7	1.3	35	45	460	3.7
G-V	JSC	13	2.8	45	51	440	6.0
High Altitude Stratospheric							
WB-57f (f)	JSC	6.5	4.4	36	60	410	2.5
Global Hawk (g)	AFRC	30	0.8	13	65	345	11.0
ER-2 (h)	AFRC	12	2.5	20	70	410	5.0

(a) https://airbornescience.nasa.gov/aircraft/C-130H_Hercules

(b) https://airbornescience.nasa.gov/aircraft/P-3_Orion

(c) https://airbornescience.nasa.gov/aircraft/DC-8

(d) https://airbornescience.nasa.gov/aircraft/C-20A_G-III_-_Armstrong

(e) https://airbornescience.nasa.gov/aircraft/G-III_-_JSC

(f) https://airbornescience.nasa.gov/aircraft/WB-57

8.3.1. Heavy lift troposphere

Because the volcanic plume is mainly found in the lower stratosphere, the tropospheric aircraft must be able to carry large mass and volume remote sensing instruments (e.g., lidars). This limitation largely eliminates the Ikhana and G-III's from consideration as remote sensing platforms. The C-130, P-3, DC-8, and G-V provide a heavy lift capability as platforms.

The range of the DC-8 and G-V would be able to do hemispheric-scale flights that would allow detailing of the volcanic plume's structure. Figure 8 displays a simulation of the spread of Mt. Pinatubo- and Cerro Hudson-like eruptions at 70 hPa (18 km), respectively. The plume is zonally well mixed, but has a latitude scale of 30-50°. Hence an aircraft sited somewhere near the plume would need a range exceeding this scale (1800-3000 nmi). While the C-130 and P-3 have ranges greater than 3000 nmi, the DC-8 and G-V both provide considerable range margins when considering operational issues (FIR restrictions, etc.) and uncertainties in model predictions.

The NASA DC-8 has been the primary aircraft for many science campaigns over the last few decades and is seasoned for international operations. Many scientific instruments have previously deployed on the DC-8. Hence, the infrastructure for a rapid integration onto the DC-8 is in place. The G-V is new to the ASP fleet, and would require

Table 11: Heavy lift tropospheric payload

Instrument	Acronym	Measurements	AC	Type	Org	Contact Person
Fourier Transform Infrared Spectrometer	FTIR	Column	DC-8	Spectrometer	NCAR	Jim Hannigan
Gas and Aerosol Measurement Sensor/Langley Airborne A-Band Spectrometer	UV DIAL/ HSRL	O_3, Particulate backscatter, particulate extinction, particulate depolarization	DC-8	Lidar	LaRC	Johnathan W. Hair
High Spectral Resolution Lidar – Gen 1	HSRL-1	O_3, Particulate backscatter, particulate extinction, particulate depolarization	P-3	Lidar	LaRC	Chris Hostetler
Spectrometers for Sky-Scanning, Sun-Tracking Atmospheric Research	4STAR	Aerosol Optical Depth, Water Vapor	DC-8	Spectrometer	ARC	Jens Redemann
Gas & Aerosol Monitoring System/ Langley Airborne A Band Spectrometer	GAMS/LA ABS	Optical Depth	DC-8	Solar Occultation, Spectrometer	LaRC	Michael Pitts
High Spectral Resolution Lidar - Gen 2	HSRL-2	Particulate Backscatter, Particulate Extinction, Particulate Depolarization	P-3, C-130	Lidar	LaRC	Chris Hostetler

considerable work that would preclude its initial use in a rapid response time frame of less than 2 months.

8.3.2. High altitude stratosphere

In-situ observations of the volcanic plume are crucial to understanding and modeling the Earth system response. Figure 7 shows the simulated vertical evolution of a Pinatubo-like aerosol cloud, from which we infer that the minimum altitude for the aircraft is 18 km. Hence, the ER-2, WB-57, and Global Hawk would all be sufficient platforms for observing the plume.

While the ranges of the platforms suggest that the Global Hawk is the best option, with its 11,000 nmi. range covering latitudes from the North Pole to the SH subtropics, this aircraft has limited deployment and payload capabilities. The Global Hawk could be used in the SH with the Global Hawk Mobile Operations Facility (GHMOF) and a mobile payload facility, but this requires an extended shipping period and set-up.

The WB-57f has an outstanding payload capability, exceeding 8,000 lbs. Furthermore, the WB-57f also has flown a large number of Earth Science instrumentation over the 20 years, and is relatively easy and fast to integrate onto. However, the WB-57f
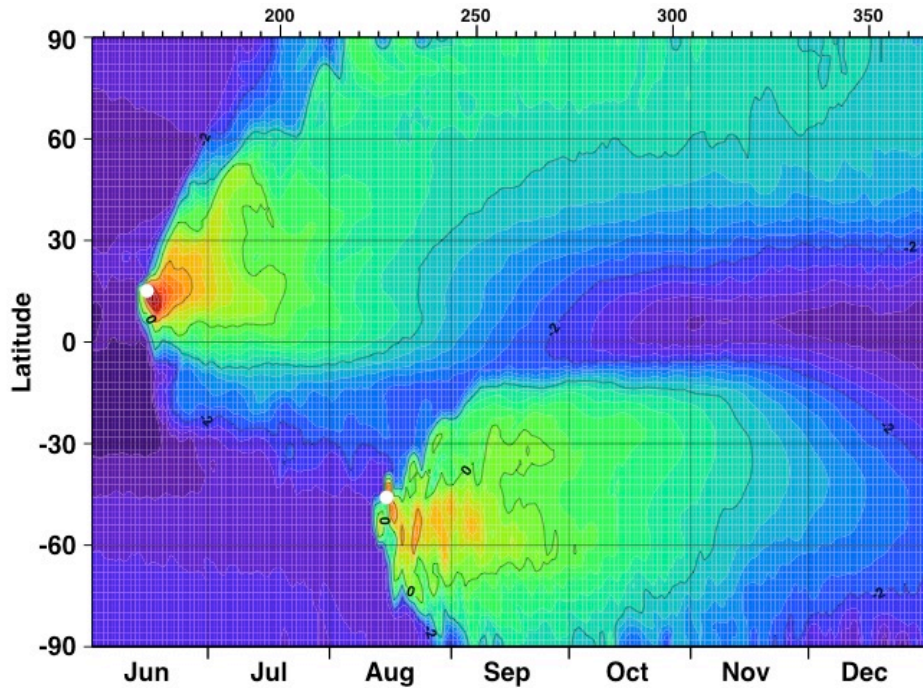
Figure 8: Latitude versus time plot of simulated SO₂ concentration following an eruption of Mt. Pinatubo in mid-June, and Cerro Hudson in mid-August (marked by white dots). Concentrations are plotted on a log scale, where the value -2 represents 0.01 ppbv of SO₂.

has only a maximum altitude of about 62 kft and is the most limited in range of the high-altitude platforms.

The ER-2 has a long history with NASA Earth science missions. The NASA U-2 sampled the Mt. St. Helens plume within 24 hours after the major eruption of 18 May 1980. The ER-2 has the highest operational altitude of the NASA aircraft, and has a good range capability (5,000 nmi). Integration on the ER-2 is more difficult than on the WB-57f, but also has an excellent record of supporting stratospheric sampling in-situ missions.

One of the primary limitations on the current high-altitude NASA aircraft is the lack of studies on the impact of ash on the engines. Generally, the larger ash particles settle out of the stratosphere within a few days (Self, 2006), but studies on the aircraft are necessary from a safety standpoint for volcano plume sampling.

Table 12: High altitude payload

Title	Acronym	Measurements	AC	Type	Org	Contact Person
Ultra High Sensitivity Aerosol Spectrometer	UHSAS	Aerosol Size Distribution & Concentration	GH	Spectrometer	LaRC	Luke Ziemba
Diode Laser Hygrometer	DLH (maybe HCl too)	H_2O	WB-57	Laser absorption	LaRC	Glenn S. Diskin
Whole Air Sampler	WAS (NCAR)	NMHCs, Halocarbons	ER-2, WB-57	WAS	U. Miami	Elliot Atlas
Dual-Beam UV-Absorption Ozone Photometer	NOAA O3	O_3	ER-2, WB-57	Photometer	NOAA	Troy Thornberry
Sulphur Dioxide	SO2	SO_2	WB-57	LIF	NOAA	Drew Rollins
Meteorological Measurement System	MMS	Wind,temp., position	ER-2	In-situ	ARC	T. Paul Bui
Solar Spectral Flux Radiometer	SSFR	Solar flux, Irradiance	ER-2	Radiometer	U. Colorado	Sebastian Schmidt
Broad Band Radiometer	BBR	Total broadband	ER-2	Radiometer	NRL Monterey	Anthony Bucholtz
Cavity Ringdown		Aerosol Optical Depth	P3		NOAA	Ru-Shan Gao
Quantum Cascade Laser System	QCLS	CO_2, CO, CH_4, N_2O	WB-57	Laser absorption	Harvard U.	Bruce Daube
Chemical Ionization Mass Spectrometer	NOAA CIMS	H_2O, HNO_3, HCl	WB-57	CIMS	NOAA	Ru-Shan Gao
Chemical Ionization Mass Spectrometer	GIT-CIMS	BrO, HOBr + Br_2, N_2O_5	ER-2, WB-57	CIMS	Georgia Tech	Huey
Multi-AXis Differential Optical Absorption Spectroscopy	CU-AMAX-DOAS	BrO, NO_2		Passive Remote Spectrometer	U. Colorado	Volkamer
Chemiluminescence	HU	ClO, possibly BrO	ER-2, WB-57	Chemiluminescence	Harvard	Anderson
NCAR NOxyO3	NOxyO3	NO, NO_2, NO_y, O_3	WB-57	Chemiluminescence	NCAR	Andrew Weinheimer
Particle Analysis By Laser Mass Spectrometry	PALMS	Particle composition, aerosol	WB-57	Spectrometer	NOAA	Karl Froyd
Nuclei-Mode Aerosol Size Spectrometer	NMASS	Particle size distribution, condensation nuclei	ER-2, GH, WB-57	CN counter, Spectrometer	LaRC	Luke Ziemba

8.4. Deployment sites

The volcanic eruption plumes tend to mix zonally on a relatively short time scale of 1 month (see Appendix 3). Hence, airfield basing locations are not needed at multiple locations in latitude and longitude, but spaced in latitude to provide pole-to-pole coverage. The airfields were chosen based upon relatively recent experience by NASA at those locations with our ASP aircraft. The sole exception to this is Lima, Peru. The first deployment should occur at approximately the same latitude of the volcanic eruption.
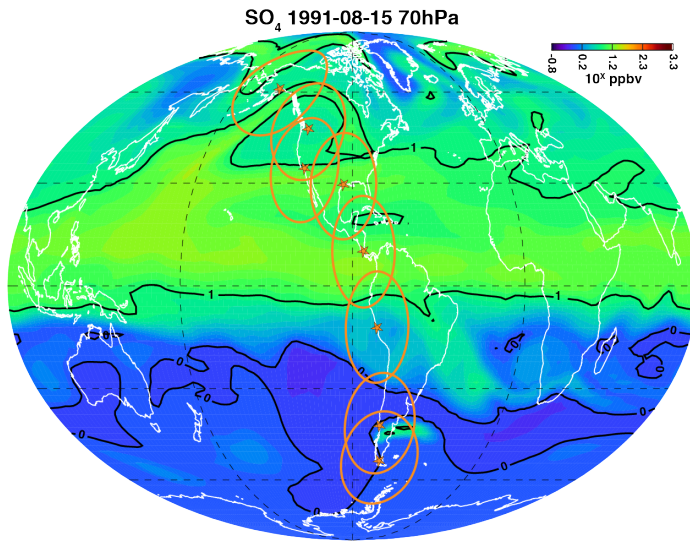
Figure 9: Map of simulated total SO₄ (vapor and aerosol) at 70 hPa (~18 km) on 15 August 1991 following a mid-June and a mid-August eruptions such as the ones of Mt. Pinatubo and Cerro Hudson. Concentrations are plotted on a log scale, where the value 1 and 0 respectively are 10 and 1 ppbv of total SO₄ (color scale on top right). Aerodrome locations are orange.

The aircraft must be able to sample over broad latitudinal scales because of the plume's dispersion in latitude. Figure 9 shows a set of aircraft base locations that would provide pole-to-pole coverage (see Table 15). The 1800 km range rings on Figure 9 are based upon the effective operational range of a WB-57f straight line out-and-back style flight with a few vertical profiles of the lower stratosphere.

The deployment sites shown here have varied logistics pros and cons. Appendix B shows details of these sites with some of the logistic problems.

8.5. Timeline

There are two timelines to consider for sampling a volcanic plume. First, it is a primary requirement to estimate the initial plume injection altitude and to capture the total injected mass of SO_2. Because the SO_2 is oxidized in the stratosphere by the hydroxyl radical, the SO_2 mass decays with an e-folding time scale of ~1-2 months (see Appendix C). Hence, the initial aircraft deployment must take place within 2 months of the eruption. Second, as the SO_2 is oxidized, it forms sulfate aerosol. The aerosol concentrations rapidly build in the stratosphere to a peak within 6 months, and then decay with an e-folding time scale of ~1 year. Hence, additional deployments are needed in the later years at approximately 1, 2, and 3 years following the eruption. These later year deployments should be staged from airfields in both hemispheres because of the strong plume dispersion across the stratosphere.

The first timeline for an aircraft deployment is in the immediate aftermath of a major eruption (see Figure 10).The deployment is a race between getting sulfur dioxide, sulfate, and particle instruments airborne, and the rapid drop-off of SO_2 from OH oxidation, and the dilution of possible halogen injection. If a major event occurs, the response will evolve according to the attached timeline.

- Day 0: Eruption occurs
- Day 3: Satellite's verify a major eruption
- Day 14: HQ agrees, assets re-tasked (& instruments).
- Day 28: Aircraft are ready for integration, and PIs arrive on site
- Day 49: Transit to base
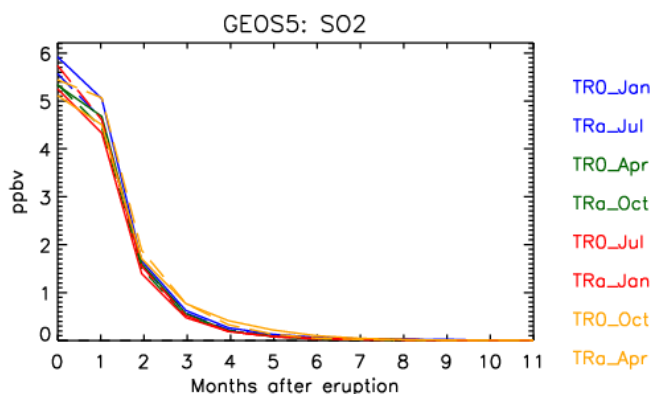- Day 56: Science flights begin

Figure 10: Modeled mean stratospheric volcanic SO2 mixing ratio tropical. Dashed lines indicate southern hemisphere eruptions, and colors indicate the season of the eruption, depending on the hemisphere.
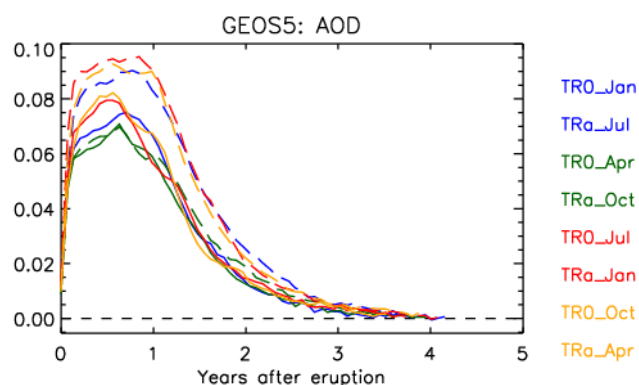

Figure 11: Similar to Figure 10, but showing the perturbation to the global mean AOD [550 nm] following the eruptions.

Additional deployments would be timed and spaced according to the plume's evolution. Figure 11 displays the evolution of the global mean aerosol optical depth. A second deployment would be staged to capture the peak concentration of sulfate aerosol at approximately 9 months after the eruption, with third and fourth deployments at the 18 and 27 month points. These additional deployments would be used to clearly define the exponential fall-off of the aerosol loading and the evolution of the size distribution.

One of the major conundrums of the Mt. Pinatubo eruption was the strong perturbation of the nitrogen chemistry without a comparable depletion of ozone. This discrepancy was eventually resolved with careful differentiation of model simulations that showed that the ozone depletion had been masked by atmospheric transport (Aquila et al., 2013). This suggests that the deployment around the peak of the sulfate aerosol ought to include deployments in both hemispheres. The model simulations (see Appendix C) suggest that if the eruption occurs in the mid or high latitudes, than a deployment to the other hemisphere may not be necessary.

Finally, it has long been known that the presence of stratospheric bromine from very short lived (VSL), biogenic compounds renders the stratosphere more sensitive to depletion following a major volcanic eruption (Salawitch et al., 2005). Many model calculations of the future impact of volcanic eruptions have neglected VSL halogens. The direct injection of halogens to the stratosphere by Pinatubo was negligible (Tabazadeh and Turco, 1993). However, the direct injection of stratospheric halogens at significant levels following major eruptions is nonetheless predicted by theory (Gutiérrez et al., 2016) and has been confirmed for other, historical eruptions via ice core analysis (De Angelis et al., 2003). It is possible the lack of stratospheric injection of halogens by Pinatubo was driven by the passage of a tropical cyclone through the paroxysmal eruption plume (Tupper et al., 2005). Given the sensitivity of stratospheric ozone to VSL bromine and the direct injection of either chlorine or bromine following a future major eruption (Klobas et al., 2017), plus

of course the enhancement of ClO following heterogeneous chemistry, we are recommending the aircraft payload include ClO, HCl, BrO, and possibly related halogen species (i.e., some CIMS instruments are capable of quantifying other halogens).

9. Modeling to support a deployment

Peter Colarco (GSFC/614), Valentina Aquila (American University), Allegra LeGrande (GSFC/611), Kostas Tsigaridis (GSFC/611, Columbia University)

9.1. Introduction

There are several contributions the modeling community can make to defining and coordinating a NASA response to a major volcanic eruption. These include:

- ensembles of model simulations performed prior to an eruption in order to gauge likely transport paths and impacts of a range of possible volcanoes and eruptions. This step has already been performed. A summary of results from these simulations is in Appendix A3.
- near-real time/operational model simulations in the immediate aftermath *of an eruption* to forecast near-field plume transport (typically 5 – 10 day forecasts)
- longer-term simulations (weeks to months to years) following an eruption to estimate impacts specific to a particular eruption

It is useful to recognize that, in general, these three modeling activities may not be performed with the same modeling systems or capabilities. For example, typical operational modeling systems are run at much higher spatial resolution ($< 1°$) than models performing climate predictions. Additionally, the capabilities of aerosol and chemistry codes are often different between these classes of models, with operational models usually running simpler codes than those used in climate simulations. On the other hand, there are common needs regardless of the modeling system, including definition of the initial conditions (i.e., the atmospheric state) and estimation of the relevant injection parameters, such as plume composition (e.g., SO_2, ash, water, halogens), injection amount, timing, and vertical structure.

9.2. Preparatory actions

In order to provide guidance to NASA on how best to deploy resources following a major volcanic eruption, models can be invoked prior to an eruption to investigate the transport, evolution, and climate impact of volcanic emissions. Two NASA Earth system models recently performed a series of simulations to support NASA's volcano response: the GSFC Goddard Earth Observing System (GEOS-5) model and the GISS ModelE. Similar suites of experiments were performed with each of these models using eruption parameters compatible with the 1991 Mt. Pinatubo eruption (14 Tg of SO_2 injected between 18 km and 24 km altitude) for hypothetical eruptions occurring at different latitudes and in different seasons. This suite of simulations generalizes the impact of a Pinatubo-class eruption based on latitude and season, and should be used as an asset in pre-eruption mission planning. Details about the setup of these simulations, model descriptions, and simulation results are presented in Appendix A3.
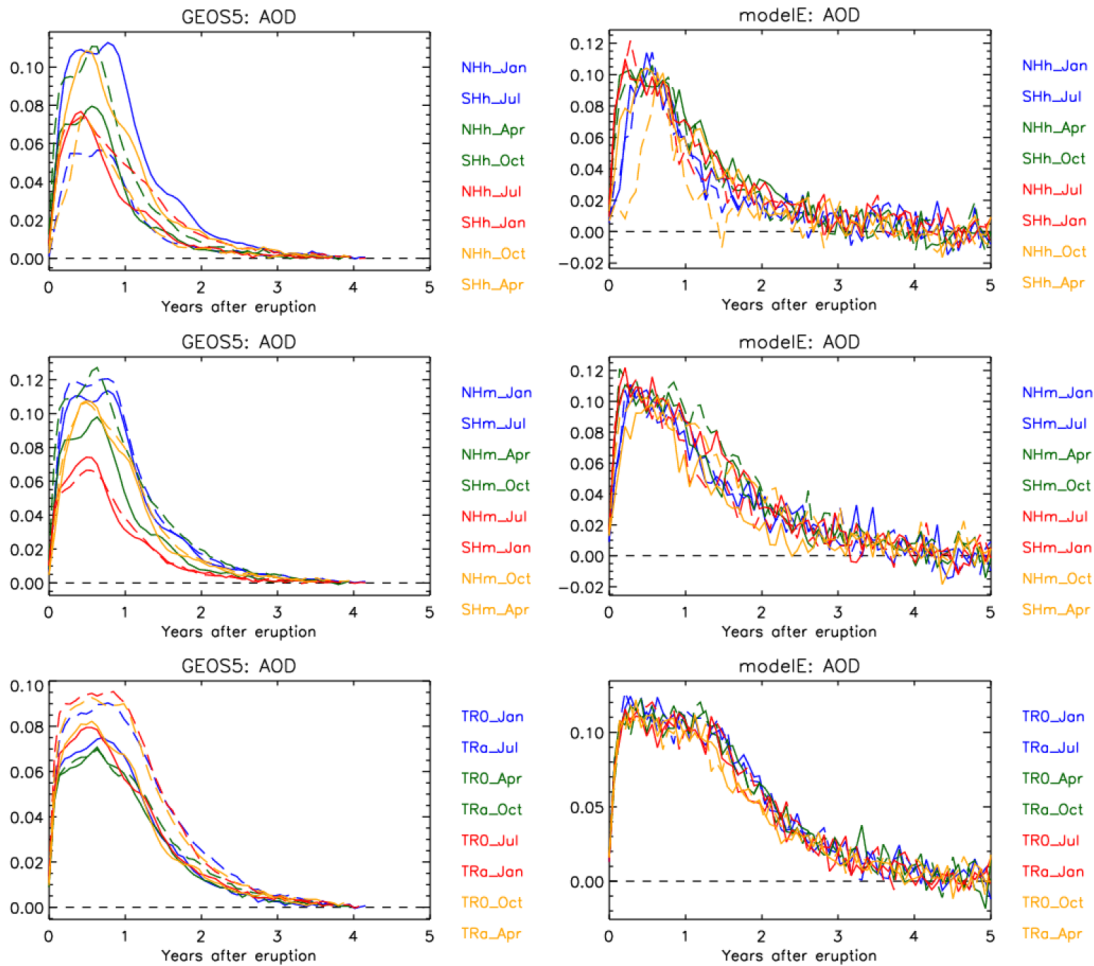
Figure 12: GEOS-5 and ModelE simulated global mean AOD for simulations of a Pinatubo-sized volcanic eruption occurring in the month indicated for each of six latitudes (NHh/SHh=Northern/Southern High Latitude, NHm/SHm = Northern/Southern Mid-Latitude, TRO/TRa=Northern/Southern Tropics)

The global mean aerosol optical depth (AOD) rapidly increases following the eruption of a Pinatubo-like volcano (see Figure 12). Individual panels are shown for each of the six eruption locations (northern/southern high latitudes, midlatitudes, and tropics), and on each panel we show the AOD evolution following eruptions that took place in January, April, July, and October. These simulations show a recovery period of the AOD to background levels of about 5 years following such an eruption. This recovery is generally faster for high latitude eruptions and slower for tropical eruptions. The peak perturbation in AOD (about $0.1 - 0.12$) of such an eruption is comparable in magnitude to the global mean AOD of tropospheric aerosols. However, the climate impact of the stratospheric aerosols is greater because there is no counteracting warming from carbon aerosols as there is in the troposphere.

Results such as the one shown in Figure 12 help identifying when to deploy over the lifetime of the volcanic aerosol in order to measure the evolution of the volcanic perturbation. Additionally, maps of AOT, sulfate, and sulfur dioxide concentrations can guide the location of the deployment. Following the timeline for an aircraft deployment

43

Table 13. ICAP near-real time/operational global aerosol models. For most models simulated species are DU=dust, SS=sea salt, SU=sulfate, BC=black carbon, and OC=organic carbon. For BSC and NOAA near-real time capabilities for BC/OC/SU will arrive soon. QO stands for quasi-operational and O for operational. CAMS is run operationally but at a 24 hour delay.

Org.	BSC	Copernicus/ ECMWF	JMA	Meteo France	NASA	US Navy	NOAA	UKMO
Model	NMMB/ BSC-CTM	CAMS	MASINGAR	MOCAGE	GEOS-5	NAAPS	NGAC	UKMO
Status	QO	O-24 hrs	QO	O	QO	O	O	O
Meteorology	Offline NMMB	Inline IFS	Inline AGCM	Offline ARPEGE	Inline GEOS-5	Offline NAVGEM	Inline GFS	Inline UM
Resolution	1.4° x 1°	0.4° x 0.4°	0.56° x 0.56°	2° x 2°	0.25° x 0.31°	0.33° x 0.33°	1° x 1°	0.35° x 0.23°
levels	24	60	40	47	72	60	64	70
DA	EnKF[p]	4DVar	EnKF[p]	Est. 2018	2DVar +LDE	2DVar 3DVar, EnKF[p]	NA	4DVar
Assimilated Obs	DAQ MODIS+ DB	DAQ MODIS+DB	CALIOP, MODIS, Himawari-8	NA	Neural Net MODIS	DAQ MODIS, CALIOP	NA	MODIS Dust AOT
Species	DU SS BC OC SU	DU SS BC OC SU	DU SS BC OC SU	DU SS BC OC SU	DU SS BC OC SU	Anthro+ bio B. Burn DU SS	DU SS BC OC SU	DU
Size Bins	8 (DU,SS) Bulk BC, OC, SU	3	10	6	5 (dust ss) Bulk BC, OC, SU	1	5 (dust ss) Bulk BC, OC, SU	2

reported in Section 7, at least 2 months are needed to start taking measurements. Our simulations indicate that 2 months after the eruption the aerosol is zonally well distributed, and the results of each model experiment indicate which latitudinal range is optimal for measurements (see Appendix A3 for details).

While the general evolution and recovery time of the volcanic AOD is similar for GEOS-5 and ModelE, the two models simulate different seasonal dependence of the AOD magnitude, possibly because of different circulation simulated in each model or because of the difference in microphysical schemes. Model discrepancy such as this identify which observations are crucial to understand the atmosphere and climate impact of a volcanic eruption.

Inviting a diversity of models to participate in such an exercise is useful in broadening the understanding of the expected response. For example, GEOS-5 and ModelE are run with different aerosol and chemistry schemes and vertical resolutions, and employ different formulations of dynamics and chemistry. This results in differences in the

Table 14: Global models able to simulate stratospheric aerosol

Model	Aerosol microph.	Het. Chem.	Rad. Interac.	Reference
CAM5/CARMA	Y	Y	Y	Yu et al. (2015)
CCSR/NIES	N	Y	Y	Takigawa et al. (2002)
CES<(WACCM)	Y	Y	Y	Mills et al. (2016)
ECHAM5-HAM-SALSA	Y	N	Y	Bergman et al. (2012), Laakso et al. (2012)
EMAC	Y	Y	Y	Brühl et al. (2015)
GEOS-5/CARMA	Y	Y	Y	Aquila et al. (2017)
GEOS-5/GOCART	N	Y	Y	Aquila et al. (2013)
ModelE+MATRIX	Y	Y	Y	Bauer et al. (2008)
MAECHAM5-HAM	Y	N	Y	Niemeier et al. (2009), Toohey et al. (2013)
MAECHAM5-HAM2	Y	N	Y	Laakso et al. (2012)
MAECHAM-SAM2	Y	N	N	Hommel et al. (2011)
MRI-ESM1	N	Y	Y	Yukimoto et al. (2011), Tanaka et al. (2003)
SOCOL-AER	Y	Y	Y	Sheng et al. (2015)
TM5	Y	Y	N	Bânda et al. (2015), van Noije et al. (2014)
ULAQ_CCM	Y	Y	Y	Pitari et al. (2014)
UKESM-LO (includes UKCA-GLOMAP)	Y	Y	Y	Morgenstern et al. (2009), Dhomse et al. (2014)
CESM(WACCM)-CARMA	Y	Y	N	Campbell et al. (2014)
MIROC-CHASER/SPRINT AS	Y	Y	Y	Sekija et al. (2016)
AER	Y	Y	N	Salawitch et al. (2005), Klobas et al. (2017)

simulated transport, lifetime, and climate impacts of the volcanic plume, which reflect the range of current model uncertainties and provide guidance on which measurement capabilities are most needed to reduce model uncertainty on the climate impacts of volcanic eruptions.

Section 6 of Appendix A3 explain in details how such simulations could be used to prepare for a deployment in the event of a major volcanic eruption. The results of these simulations are archived at the NASA Center for Climate Simulations (NCCS) and are available upon request.

9.3. Near term plan (0-1 month after the eruption)

Operational forecast models have the potential to provide guidance immediately following an eruption. There are a growing number of global forecasting centers around the world that now include aerosol and other tracers in their near-real time forecast products. Table 9 shows the capabilities of the various member models contributing to the International Cooperative for Aerosol Prediction (ICAP, Benedetti et al. 2011, Reid et al.

2011, Colarco et al. 2014) multi-model ensemble (Sessions et al. 2015). These models are all operational or quasi-operational, providing near-real time aerosol forecasting capabilities and (nearly all) invoking some form of aerosol data assimilation. Several of the models are run by modeling centers producing well-known atmospheric analyses (ECMWF, NASA, NOAA, US Navy, UKMO). Typically, the ICAP models are running at high spatial resolution (< 1°), with a focus on short-term (5- to 10-day) predictive capability.

In order to realize the immediate benefit of near-real time forecasting capabilities in the aftermath of an eruption, we need models prepared to cope with an eruption. Without directly accounting for the eruption itself the only value added from these models is to the extent that assimilation of AOD products (e.g., from MODIS) provides an estimate of the aerosol loading. This is problematic because, in the first place, without explicitly accounting for the volcanic eruption in the forward model the data assimilation step is likely to view the observations of an extreme perturbation as spurious and discard most of them. Secondly, even if the observations are somehow incorporated into the analysis, lacking an explicit volcanic injection the observations are likely to be misattributed to the wrong aerosol specie and atmospheric profile. For example, if Pinatubo were to erupt today an operational model would likely attribute the sudden increase in AOT to some mixture of mainly boundary layer anthropogenic pollution and sea salt, neither of which would provide useful forecast guidance.

The necessary step for an operational system is to be prepared to ingest information about the volcanic event itself, by incorporating it along with other emission sources into the background model. Practically this could happen by combining near-real time available observations of SO_2 loading (e.g., OMI-derived) and lidar or visual estimates of the plume height, and then providing those parameters to the model. There is additionally an active online community of data providers and modelers that follows volcanic events as they happen. Their expertise, the availability of SO_2 observations from OMI and aerosol observations from MODIS and CALIOP, and the observational guidance provided to aviation authorities by the Volcanic Ash Advisory Centers (VAACs), suggest that most of the information needed to determine injection parameters already exists. The ability to provide this information as a cohesive set of parameters in near-real time to modeling communities, however, has not to our knowledge been exercised. Additionally, there needs to also be a "concept of operations" that would allow the model to cope with such an event. For example, the forecasting center could allow the possibility to run a parallel stream of their system that starts from the analysis state immediately prior to the eruption but includes a source term for the eruption. This parallel stream would run until it caught up to the main model stream (the one that did not have eruption parameters) and then replace it as the operational stream that propagates forward. This is the notional concept of operations at the GMAO, but it has not been exercised yet, and to our knowledge there are no modeling centers currently prepared to do this kind of thing in anything other than an *ad hoc*, best effort sense. Climate models (e.g., GISS ModelE) could potentially provide near-real time forecast guidance by initializing simulations from operationally provided meteorological analyses. Alternatively, climate models could be run for a long period of time and then this control could be mined to find the initial conditions most closely resemble the observed atmospheric state at the time of an actual eruption; this approach has the benefit of providing initial conditions more attuned to the particular climate model than any set of atmospheric analyses could provide.

9.4. Long term plan (>1 month after the eruption)

To investigate the longer-term impacts of an actual eruption we resort to the same sorts of models being used to provide prior-eruption guidance. The distinction here is that, following an eruption, we will have in the near-term estimates of the eruption parameters (injection composition, amount, timing, and location, including altitude) as well as initial conditions of the atmospheric state from analyses. Table 14 summarizes the capabilities of global three-dimensional models capable of simulating stratospheric aerosols, as compiled by Kremser et al. (2016). Both the GSFC and GISS models are ready to simulate an eruption of known parameters and estimate its medium- to long-term evolution. Given the availability of analyses from the near-real time GMAO GEOS-5 system it is possible to provide initial conditions to either model essentially immediately in the aftermath of an eruption.

10. Appendix 1: Lidar Network Supporting Material

MPLNET utilizes small, low-powered, eye-safe lidars. Lidar detection capabilities are most often reported in terms of the scattering ratio: the ratio of total backscatter (molecular + aerosol) to molecular backscatter. A value of 1 indicates a clean background molecular atmosphere free of particles. The health of the lidar instrument (laser, optics, etc.) and environmental parameters (low fog, heavy aerosol or cloud loading) all affect the resulting SNR profile obtained from the instrument. A lower SNR at a given altitude will increase the minimum scattering ratio that is detectable at that altitude. The purpose of this Appendix is to demonstrate the scattering ratio detection limits of MPLNET for volcanic aerosol layers expected to be encountered from weak (VEI 3-4) to strong (VEI > 4) eruptions.

MPLNET has demonstrated the ability to detect and provide useful data products to track and analyze stratospheric aerosols. Campbell et al. (2009) present long-term observations of polar stratospheric clouds (PSC) at the South Pole. Results from that study are shown in Figure 13, where PSC attenuated scattering ratios are displayed. Here the scattering ratio profiles have not been corrected for attenuation by lower aerosols. Hence the true scattering ratios will be higher than those shown here near the top of the PSC layers. The data show that MPLNET was capable of detecting weak PSC layers with scattering ratios as low as ~1.2. Sawamura et al. (2012) utilized MPLNET, together with other lidar networks and CALIPSO, to track and analyze aerosol plumes from the Nabro volcanic eruption in 2011 as they propagated worldwide. The Nabro eruption was considerably weaker (VEI 3-4) than Pinatubo (VEI 5-6), and did not have a significant climatic impact despite plume layers lingering for several months. As a result, the ability of MPLNET to detect and track the Nabro plumes provides a baseline for detection capability. It would be easier to detect plumes from larger eruptions (VEI +4). Figure 14 shows results from Sawamura et al (2012) of the Nabro scattering ratios obtained from MPLNET, EARLINET,
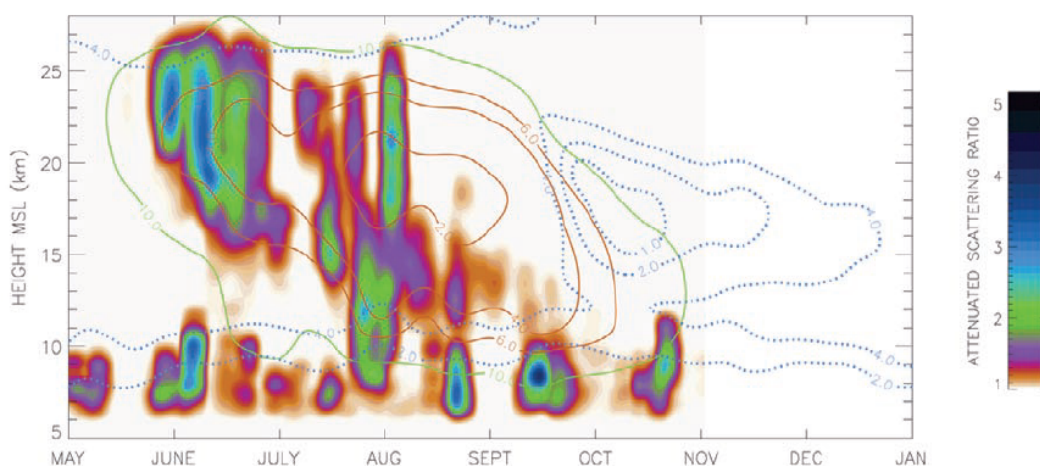

Figure 13: Profiles of polar stratospheric cloud attenuated scattering ratios from long-term observations at the MPLNET South Pole site (from Campbell et al., 2009).
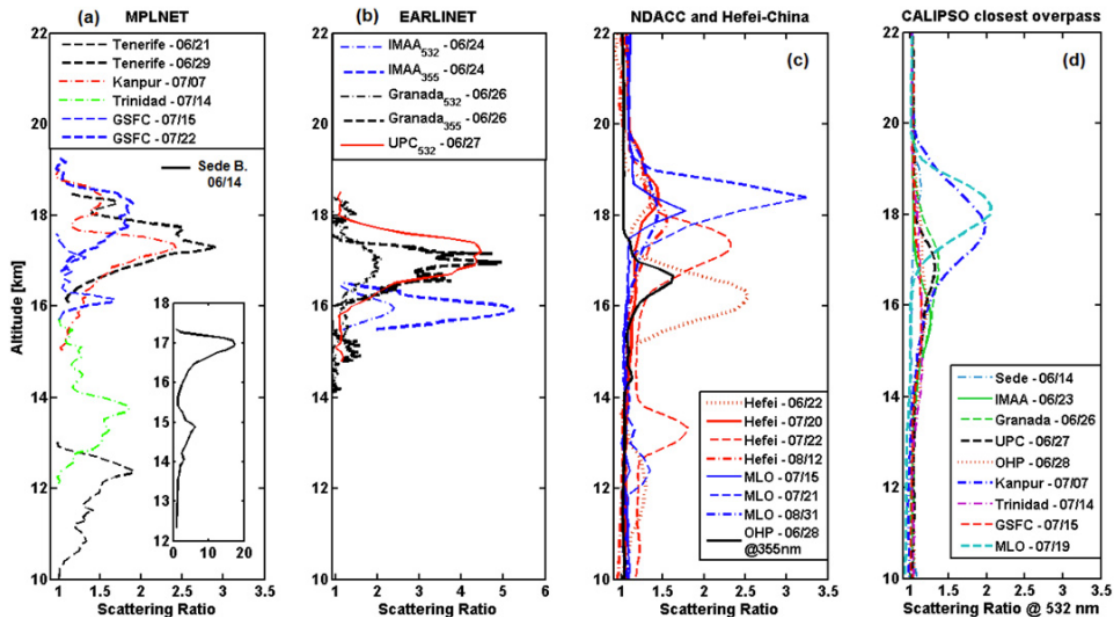
Figure 14: Profiles of volcanic aerosol scattering ratios from the Nabro 2011 eruption obtained from MPLNET, EARLINET, NDACC, and CALIPSO measurements (from Sawamura et al. 2012).

NDACC, and CALIPSO over the course of the first month post-eruption. MPLNET is clearly capable of detecting weak volcanic layers with scattering ratios lower than 1.5, and produces similar results to those from the other more powerful lidars. These results provide evidence of a baseline MPLNET scattering ratio of ~1.2, similar to the PSC findings from Campbell et al. (2009).

MPLNET data have contributed to other volcanic aerosol studies. Fromm et al. (2014) utilized MPLNET data in conjunction with other sources to revisit the aerosol impact from the Nabro 2011 and Sarychev Peak 2009 eruptions. Campbell et al. (2012) used MPLNET data to study the seeding of cirrus clouds from volcanic aerosols emitted from the 2008 Kasatochi eruption. However, none of these studies addresses the measurement conditions expected in the event of a large eruption. The scattering ratios would be much larger than the minimum detection limit of MPLNET. But the plume will be higher, reaching deep into the stratosphere with lower expected SNR. The layers will also persist much longer in the stratosphere, and weaken with time. Here we address the ability of MPLNET to detect and track such plumes during the first year and beyond.

Vernier et al. (2011) presented a comprehensive review of stratospheric volcanic aerosol impacts in the tropics from 1985 to 2010. One aspect of the study utilized SAGE II and CALIPSO data to construct profiles of a product they termed the stratospheric aerosol extinction ratio: the ratio between aerosol and molecular extinction. The data presented were monthly mean extinction ratios from 20°S to 20°N. The results from Vernier et al. were later expanded upon by Kremser et al. (2016), where they extended the aerosol extinction ratio profile data through 2012 and provide a corresponding plot of stratospheric aerosol optical depth. Both studies correlate the stratospheric aerosol data with significant volcanic eruptions. The top panel of Figure 15 shows the results from Kremser et al. (2016). The two letter symbols along the time axis represent volcanic

eruptions presented in their work. The original image from Vernier et al. provides contour lines with numeric value to obtain the actual extinction ratios within the layers. These results provide a view of the impact from major eruptions and the variation of the measurement scenarios likely in the months and years after. However, the data are presented as extinction ratios, not scattering ratios more commonly used for lidar. The
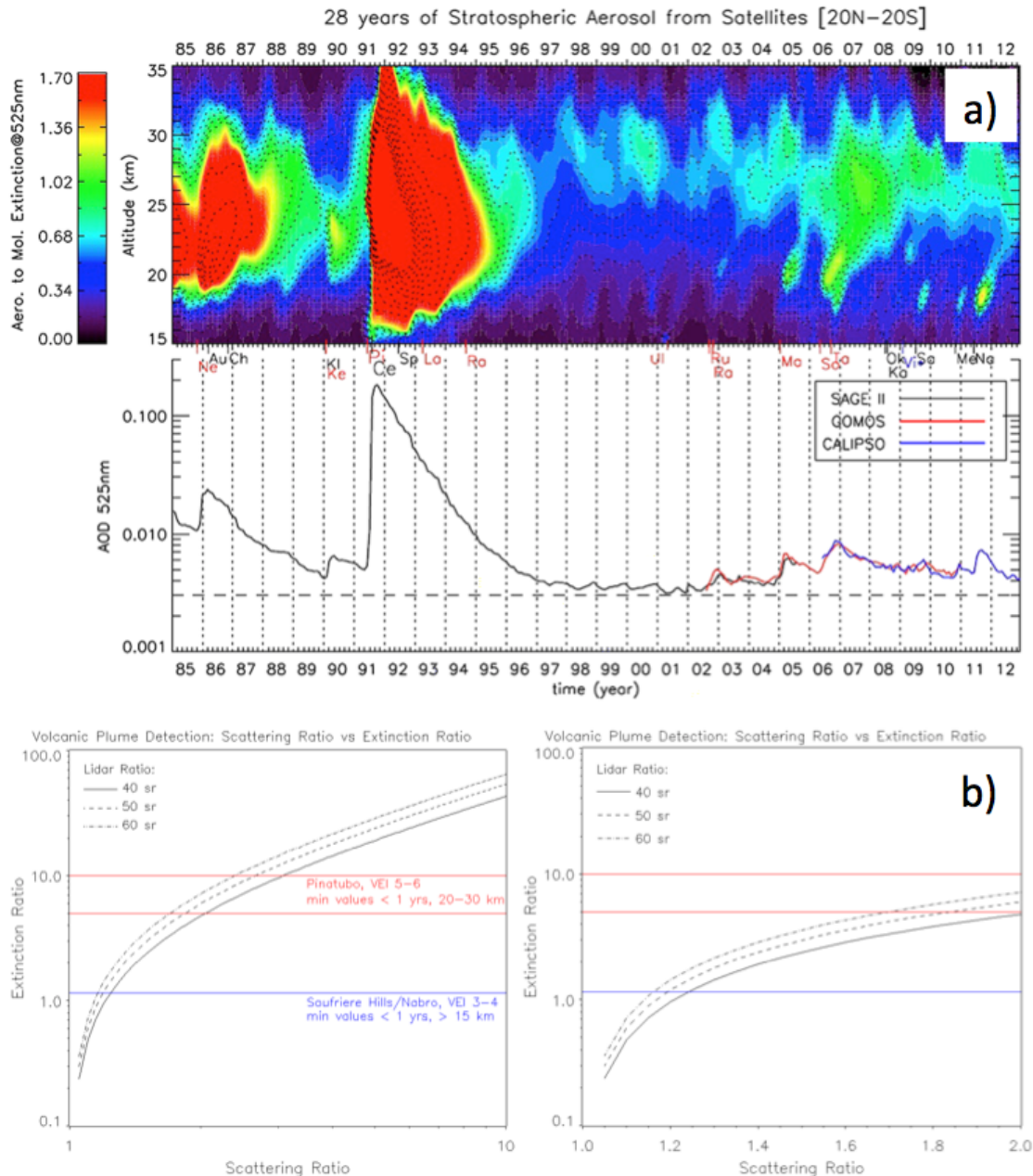

Figure 15: Top panel (a) depicts stratospheric aerosol extinction ratio and optical depth at 525 nm from SAGE II, GOMOS, and CALIPSO with key volcanic eruptions identified along the time axis (Kremser et al. 2016). The bottom panel (b) presents plots of scattering ratio vs extinction ratio for the range of lidar ratios expected for volcanic aerosol. The minimum extinction ratios for weak (VEI 3-4) and strong (VEI 5-6) volcanic eruptions were obtained from the Kremser et al. and Vernier et al. data, and are superimposed on the plots in panel (b).

relationship between extinction ratio and scattering ratio is dependent upon the aerosol lidar ratio (an intensive property of the aerosol dependent upon the particle phase function at 180 degrees and single scatter albedo, and is the ratio of extinction to backscatter). The bottom panel of Figure 15 shows the relationship between scattering ratios and extinction ratios for the range of lidar ratios expected for volcanic aerosol.

Extinction ratios associated with plumes from the following eruptions were inspected: Nevado del Ruiz (Ne), Pinatubo (Pi), Soufriere Hills (So), and Nabro (Na). The minimum extinction ratios present within the bulk of each plume (from 15-30 km) during the first year after each eruption were determined from the data presented by Vernier et al. and Kremser et al. Soufriere Hills and Nabro are representative of weak isolated eruptions (VEI 3-4) producing weak stratospheric aerosol layers over the first year. The minimum extinction ratio for Soufriere/Nabro ranged from 1.1 to 1.2, which equates to a scattering ratio of ~1.15. It is important to note that the maximum extinction ratios from these eruptions are only ~1.3. These values were derived from monthly means across a 40° latitude band. As a result, they do not capture the more concentrated portions of the plumes as reported in the month after the Nabro eruption (Sawamura et al., 2012). Scattering ratios from 2 – 10 were measured, equating to extinction ratios over 5. Despite these findings being derived from large area monthly means, they do serve as a useful baseline for the minimum scattering ratios required to detect and track the plumes worldwide, not just along the primary advection route. Thus, a lidar must be capable of detecting a stratospheric layer with scattering ratio on the order of 1.15 in order to provide useful data to track weak eruptions worldwide during the first year. Lidars located more along the plume path would have a higher minimum scattering ratio requirement of ~1.3 or more. These results agree with our assessment of the detection capability of MPLNET to detect and track stratospheric aerosol layers from the Nabro eruption. Data indicate that MPLNET, and thus GALION (with more powerful lidars) would be capable of tracking plumes from VEI 3-4 category eruptions throughout the first year. Some GALION lidars will be able to provide observations for weaker eruptions beyond the first year.

Pinatubo is representative of a strong (VEI 5-6) eruption, producing high levels of stratospheric aerosol during the first year with significant amounts still present years after. The minimum aerosol extinction ratio for the Pinatubo eruption was determined to be about 10 during the first year and only dropping to about 1.5 three years later. The corresponding scattering ratios associated with these values are 2.5 and 1.3 respectively. The scattering ratios only drop to about 1.2 by year four (on the order of VEI 3-4 eruptions). As stated earlier, these are minimum extinction ratios for the monthly mean 40 latitude means, actual plume values shortly after the eruption were much higher. The Cerro Hudson eruption only a few months later than Pinatubo was also a category VEI 5-6, therefore the minimum aerosol extinction ratios attributed to Pinatubo from the Vernier et al. and Kremser et al. data are likely heavily influenced by Cerro Hudson (perhaps twice as large). Even halving the minimum aerosol extinction ratio associated with Pinatubo during the first year would only drop the scattering ratio to about 1.8 which remains significantly higher than the baseline ~1.15 – 1.3 value for VEI 3-4 eruptions. Surface lidars would have no problem detecting and tracking aerosol layers from strong VEI +5 eruptions during the first year. It is not possible to determine the minimum extinction ratio from only Pinatubo for out years 2-4 from this data set due to the subsequent eruptions of Spur (1992), Lascar (1993), and Rabaul (1994) which likely elevate the background (minimum) aerosol loading during this

time. As a result, the length of time beyond 1 year that MPLNET could contribute meaningful profiling of stratospheric aerosol layers from an isolated Pinatubo scale eruption is inconclusive from these data sources. Since the values are based on the monthly large area means, it is likely that MPLNET will still provide useful profiling through at least year 2.

Vernier et al. incorrectly describe Nevada del Ruiz as a VEI 4-5 eruption. However, numerous available online sources indicate it was much weaker at VEI 3-4. The Soufriere Hills and Nabro eruptions were similar in strength (VEI 3-4) but produced a much weaker stratospheric aerosol signature in the data, illustrating the difficulties associating eruption strength with aerosol impact and discriminating the effects from multiple eruptions. Nevada del Ruiz was chosen as representative of a weaker eruption (VEI 3-4) occurring several years after a strong eruption, in this case El Chichón (VEI 5-6) in 1982 (four years prior). The goal here is to determine if MPLNET could detect the signature of a weak eruption (VEI 3-4) following a strong one (VEI +5). The Augustine (Au) eruption (VEI 3-4) occurred only 4 months after Nevada del Ruiz. Limiting analysis to the preceding 4 months indicates the eruption of Nevada del Ruiz alone clearly elevated the aerosol extinction ratios relative to the baseline values lingering from El Chichón. If one considers a background El Chichón extinction ratio of about 1 – 1.5 (from the data), then the minimum extinction ratio from Nevada del Ruiz alone would be approximately 1 (close to the Soufriere Hills and Nabro values). The Nevada del Ruiz eruption increased the stratospheric aerosol optical depth from the El Chichón background value by only 0.01. Based on examination of the post-Pinatubo period, the subsequent weaker eruptions from Spur, Lascar, and Rabaul in the following three years are barely visible in the SAGE II data. Based on these examples, it is unclear if a scattering ratio increase of 1 and associated optical depth increase of only 0.01 would be high enough for MPLNET to distinguish the signatures of a weak eruption 2-4 years after a strong one. It is likely that other more powerful lidars in GALION will have a better chance at doing so. Spaceborne lidars would have the best opportunity for such work as their SNR is highest in the stratosphere and lowers towards the surface (opposite to surface lidars). Despite limitations presented above, surface lidars would still provide layer detection and tracking data for studying multiple eruptions. The locations of the observed layers would aid model assimilation studies that would better determine the impact from the individual eruptions.

11. Appendix 2: Airfields
1. NORTHERN HEMISPHERE
1a. Sweden: Kiruna. Kiruna Airport (KRN)
1b. USA: Anchorage, AK. Ted Stevens International Airport (ANC) or Elmendorf AFB (EDF).
1c. USA: Moses Lake, WA. Grant County International Airport (MWH)
1d. USA: Palmdale, CA (AFRC)
1e. USA: Ellington Airfield, Houston TX. (JSC).
1f. USA: Guam. Antonio Won Pat International Airport (GUM) or Andersen AFB.
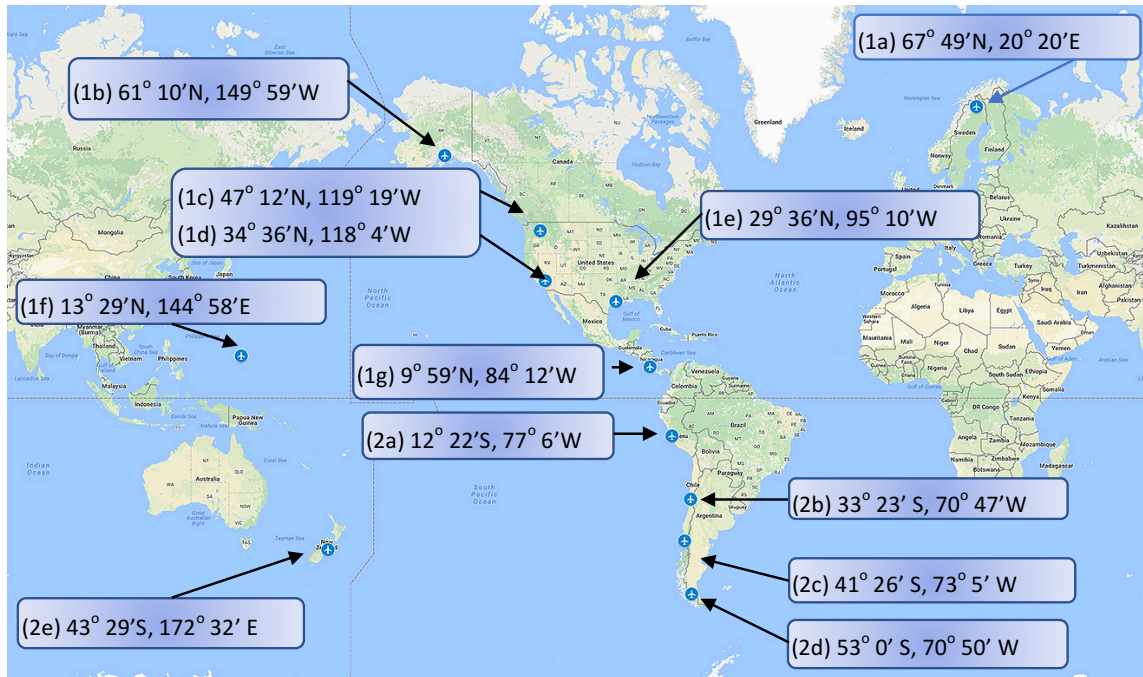1g. Costa Rica: San Jose. Juan Santamaria International Airport (SJO).

Figure 16: Possible airfields for an aircraft deployment.

2. **SOUTHERN HEMISPHERE**

    2a. Peru: In Lima: Jorge Chavez International Airport (LIM). Also, in Piura: Capt. Guillermo Concha (PIU) (5° 12' 24"S, 80° 36' 59"W) and in Arequipa: Rodriguez Ballón International Airport (AQP) (16° 20'26" S, 71° 34' 12" W). It should be mentioned that another venue could be explored for possible use: The Peruvian Air Force Base of Las Palmas (in Lima). The facility is a training base for air force cadets and it is not as busy as LIM.

    2b. Chile: In Santiago International Airport (SCL). Also to the north: In Arica, Chacalluta International Airport (ARI) (18° 20'S, 70° 20'W) or in Antofagasta International Airport (ANF) (23° 26' S, 70° 26'W)

    2c. Chile: Puerto Montt International Airport (PMC)

    2d. Chile: Punta Arenas International Airport (PUQ)

    2e. New Zealand: Christchurch International Airport (CHC)

11.1. Diplomatic clearances

A diplomatic clearance is required for each foreign country. The Office of International and Interagency Relations (OIIR) states that there is no guarantee that we will receive approvals for requests on a very short notice. Close coordination with the State Department and appropriate US embassy will be critical once the mission is authorized. The usual timeline is 3-4 months. Each country has a different process and the length of time for the approval will vary not just by country but also by their respective staffing, political climates, etc.

NASA has worked and received clearances from all of the countries listed above, many times in less than 3-month time. For example, during a deployment to Chile – and

with help from the State Department - we were able to obtain diplomatic clearance for Argentina (for one of our possible divert sites) within two weeks.

One option would be to keep a rolling agreement/clearance going with every country, but it would be time consuming, we might get negative answers given the open-ended nature of the mission. The volcanic event would actually serve to look at our expedited request more favorably and increase our odds.

11.2. Hangar availability

Neither the DC-8 nor the WB-57 aircraft require a hangar for operations, but some of the instruments on the WB-57 often require a hangar. The ER-2 aircraft does require a hangar. It is unlikely to obtain a guarantee of hangar availability for extended periods of time at any of these sites, whether commercial or military. It is to our advantage to determine hangar availability right away and/or select aircraft that have the flexibility of operating without a hangar if necessary. For example, in the past, the ER-2 and WB-57 have both operated out of Costa Rica. The ER-2 (with its wings folded) fit in the Presidential hangar, while the WB-57 required the setup of a temporary hangar for flight operations. Building a temporary hangar will add additional:

- Cost (purchasing, shipment to site, setup, removal, return shipment, additional support such as power, A/C, etc.)
- Lead time: authorization from airport authority to setup temporary hangar, purchasing contract, manufacturing, shipping, setup time. Purchase contracts alone would make this an impractical solution.

11.3. International airports vs. military/civilian airfields

Operating the ER-2 out of heavily transited international airports will present additional challenges due to the need to stop traffic of arriving/departing aircraft for ER-2 launch/recovery operations. For example, in airports such as Lima, a single runway for arrival/departure would make it extremely difficult given the high flow of traffic. The same situation would not be true in Puerto Montt (also with a single runway).

Depending on the location, access through most international airports would require additional time for mission personnel, they would have to go through airport controls every time to access the aircraft. Many times, working with an FBO will alleviate this requirement, at many locations this might not be possible to avoid.

While initially working out the authorization to work out of a civilian or military airfield may take longer than that of an international airport, operating out of an airfield might be preferable due to the easier routine access for the operations that follow. Again, advance agreement could make airport security and support services respond more quickly than waiting for the event to happen.

11.4. Northern Hemispheric sites

The US and Sweden sites have hangars suitable to house the ER-2, if available. Both Costa Rica and Sweden have been used as foreign deployment sites with the ER-2 and/or WB57 in the past (again, a portable hangar had to be setup for the WB-57 in Costa Rica).

11.5. Southern Hemispheric sites

Hangars are scarcer in the southern hemisphere. Of the sites listed they are available in Christchurch, New Zealand and Santiago (Chile). In Lima (Peru) hangars may be available for emergency work and short time use (< 24 h). At the other locations in Peru and Chile, hangars are not available. It is conceivable that temporary hangars can be setup for our operations (see notes about temporary hangar implications above).

11.6. Shipping

Of all the sites, Kiruna (Sweden) may present challenges or delayed sea shipments during the winter months. Punta Arenas (Chile) usually requires 6-8 weeks for sea shipments. Once a decision is made, shipping should occur immediately, specially of any hazmat (cannot be shipped by air) and/or low freeze point fuel for WB-57/ER-2 if necessary. Air shipments to some of these locations (PUQ for example) can still take at least a week. Once all mission cargo is defined (it will vary according to instrumentation and on-site available logistics), the cost/risk must be done to assess the feasibility of chartering an aircraft (NASA aircraft or military lift?).

11.7. Mission personnel access to deployment airports

Every site presents unique access requirements and operating conditions. ESPO has operated from most of these sites in the past (see chart below for details) and the one thing in common across every site is that all mission personnel needs to be identified and processed as early as possible, especially if personnel are from Designated Countries.

Civil servants will require official visas for Chile and Peru, no official visas are required for Sweden, Costa Rica, nor New Zealand. US Permanent residents' visitor visa requirements vary depending on their country of origin.

By 2019 all NASA personnel, including civil servants and contractors, will be required to take the High Threat Security Overseas Seminar (HTSOS), an online training session that takes anywhere from 2-5 hr to complete. The training is good for 5 years. At this time, only Costa Rica requires the HTSOS for any stay longer than 30 days. Personnel must also have passports that will not expire within 6 months of travel. Therefore, identifying probable science instruments (and their requirements) and teams in advance would be useful.

11.8. Additional comments

There are a few things that can be done to improve/help with the fast response deployment operations:
- Identify science instruments per aircraft and their required logistical needs.
- Identify personnel (at least headcount): instrument team members, crews, others.
- Visit sites without enough information. Thorough planning and assessment, in particular for the ER-2 and WB-57 aircraft support. There could be unknown factors that preclude their utilization. Need to clearly understand: access restrictions, workspace feasibility, personnel safety, aircraft security, etc.
- Visits would also help determine if we need to consider establishing multiyear rollover agreements with non-US sites.
- Keep list updated with other possible alternatives:

   o Hawaii (USA), Keflavik (Iceland), Kadena AB (Japan), Moron AB (Spain), etc.

11.9. Deployment sites' matrix

   The following table lists the sites discussed in this document. The column under each aircraft indicates the likelihood that such aircraft can operate from that site or the reason why it may not.

Table 15: Matrix of deployment sites.

Band	Coordinates	Country	Airport / AB	Prev Ops	Hangar	DC-8	ER-2	WB-57
60ºN - 70ºN	*67º 49'N, 20º 20'E*	*Sweden*	*KRN*	*Yes*	*Yes*	*Yes*	Yes	Yes
	61º 10'N, 149º 59'W	**AK, USA**	**ANC / EDF**	**Yes**	**Yes**	**Yes**	**Busy/Yes**	**Yes**
50ºN - 60ºN								
40ºN - 50ºN	47º 12'N, 119º 19'W	WA, USA	MWH		?	Yes	?	?
30ºN - 40ºN	**34º36'N, 118º 4'W**	**CA, USA**	**AFRC**	**Yes**	**Yes**	**Yes**	**Yes**	**Yes**
20ºN - 30ºN	**29º 36'N, 95º 10'W**	**TX, USA**	**JSC**	**Yes**	**Yes**	**Yes**	**Yes**	**Yes**
10ºN - 20ºN	**13º 29'N, 144º 58'E**	**Guam, USA**	**GUM / UAM**	**Yes**	**Yes**	**Yes**	**Busy/Yes**	**Yes**
0º - 10ºN	*9º 59'N, 84º 12'W*	*Costa Rica*	*SJO*	*Yes*	*No*	*Yes*	*Hangar*	*Yes*
0º - 10ºS	5º 12'S, 80º 36'W	Peru	PIU	No	No	Yes	Hangar	?
10ºS - 20ºS	12º 22'S, 77º 6'W	Peru	LIM	Yes	No	Yes	Busy	?
20ºS - 30ºS	23º 26'S, 70º 26'W	Chile	ANF	No	No	Yes	Hangar	?
30ºS - 40ºS	33º 23'S, 70º 47'W	Chile	SCL	Yes	Yes	Yes	Busy	?
40ºS - 50ºS	41º 26'S, 73º 5'W	Chile	PMC	No	No	Yes	Hangar	Yes
	43º 29'S, 172º 32'E	New Zlnd	CHC	Yes	Yes	Yes	Busy	Yes
50ºS - 60ºS	53º 0'S, 70º 50'W	Chile	PUQ	Yes	No	Yes	Hangar	Yes

Key:
- Preferred primary sites: **Bold**
- Secondary preferred sites: *italics*
- Not enough information: highlighted

12. Appendix 3: Pre-eruption simulations

Add modeling report.

13. References

Aquila, V., Oman, L. D., Stolarski, R., Douglass, A. R. and Newman, P. A. (2013), The response of ozone and nitrogen dioxide to the eruption of Mt. Pinatubo at southern and northern midlatitudes, *J. Atmos. Sci.*, *70*(3), 894–900, doi:10.1175/JAS-D-12-0143.1.

Bânda, N., M. Krol, T. van Noije, M. van Weele, J. E. Williams, P. L. Sager, U. Niemeier, L. Thomason, and T. Röckmann (2015), The effect of stratospheric sulfur from Mount Pinatubo on tropospheric oxidizing capacity and methane, *J. Geophys. Res. Atmos.*, *120*, 1202–1220, doi:10.1002/2014JD022137.

Bauer, S. E., D. L. Wright, D. Koch, E. R. Lewis, R. McGraw, L.-S. Chang, S. E. Schwartz, and R. Ruedy (2008), MATRIX (Multiconfiguration Aerosol TRacker of mIXing state): An aerosol microphysical module for global atmospheric models, *Atmos. Chem. Phys.*, *8*, 6003–6035, doi:10.5194/acp-8-6003-2008.

Benedetti, A., Reid, J. S., & Colarco, P. R. (2011), International cooperative for aerosol prediction workshop on aerosol forecast verification. *Bull. Amer. Meteorol. Soc.*, *92*(11), ES48–ES53, doi: 10.1175/BAMS-D-11-00105.1

Bergman, T., V.-M. Kerminen, H. Korhonen, K. J. Lehtinen, R. Makkonen, A. Arola, T. Mielonen, S. Romakkaniemi, M. Kulmala, and H. Kokkola (2012), Evaluation of the sectional aerosol microphysics module SALSA implementation in ECHAM5-HAM aerosol-climate model, *Geosci. Model Dev.*, *5*, 845–868, doi:10.5194/gmd-5-845-2012.

Brühl, C., J. Lelieveld, H. Tost, M. Höpfner, and N. Glatthor (2015), Stratospheric sulphur and its implications for radiative forcing simulated by the chemistry climate model EMAC, *J. Geophys. Res. Atmos.*, *120*, 2103–2118, doi:10.1002/2014JD022430.

Campbell, J. R., E. J. Welton, and J.D. Spinhirne (2009), Continous lidar monitoring of polar stratospheric clouds at the South Pole, *Bull. Amer. Meteorol. Soc.*, *90*(5), 613-617, doi:10.1175/2008BAMS2754.1.

Campbell, J. R., E. J. Welton, N. A. Krotkov, K. Yang, S. A. Stewart, and M. D. Fromm (2012). Likely seeding of cirrus clouds by stratospheric kasatochi volcanic aerosol particles near a mid-latitude tropopause fold, *Atmos. Environ.*, *46*, 441-448.

Campbell, P., M. Mills, and T. Deshler (2014), The global extent of the mid stratospheric CN layer: A three-dimensional modelling study, *J. Geophys. Res. Atmos.*, *119*, 1015–1030, doi:10.1002/2013JD020503.

Carn, S. A., K. Yang, A. J. Prata, and N. A. Krotkov (2015), Extending the long-term record of volcanic SO_2 emissions with the Ozone Mapping and Profiler Suite nadir mapper, *Geophys. Res. Lett.*, *42*, 925–932, doi: 10.1002/2014GL062437.

Colarco, P. R., Benedetti, A., Reid, J. S., & Tanaka, T. Y. (2014): Using EOS Data to Improve Aerosol Forecasting: The International Cooperative for Aerosol Prediction (ICAP). *Earth Observer*. September-October 2014.

De Angelis, M., J. Simões, H. Bonnaveira, J.-D. Taupin, and R. J. Delmas (2003), Volcanic eruptions recorded in the Illimani ice core (Bolivia): 1918–1998 and Tambora periods, *Atmos. Chem. Phys.*, 3, 1725–1741, doi:10.5194/acp-3-1725-2003.

Deshler, T., Anderson-Sprecher, R., Jäger, H., Barnes, J., Hofmann, D. J., Clemesha, B., Simonich, D., Osborn, M., Grainger, R. G. and Godin-Beekmann, S. (2006), Trends in the nonvolcanic component of stratospheric aerosol over the period 1971–2004, *J. Geophys. Res.*, *111*(D1), D01201, doi:10.1029/2005JD006089.

Dhomse, S. S., et al. (2014), Aerosol microphysics simulations of the Mt. Pinatubo eruption with the UM-UKCA composition-climate model, *Atmos. Chem. Phys.*, *14*, 11,221–11,246, doi:10.5194/acp-14-11221-2014.

Fromm, M., G. Kablick III, G. Nedoluha, E. Carboni, R. Grainger, J. Campbell, and J. Lewis, (2014), Correcting the record of volcanic stratospheric aerosol impact: Nabro and Sarychev Peak, *J. Geophys. Res. Atmos.*, *119*, 10,343-10,364, doi: 10.1002/2014JD021507.

Gao, R. S., H. Telg, R. J. McLaughlin, S. J. Ciciora, L. A. Watts, M. S. Richardson, J. P. Schwarz, A. E. Perring, T. D. Thornberry, A. W. Rollins, M. Z. Markovic, T. S. Bates, J. E. Johnson, and D. W. Fahey (2016), A light-weight, high-sensitivity particle spectrometer for PM2.5 aerosol measurements, *Aerosol Sci. Technol.*, *50*(1), 88-99, doi: 10.1080/02786826.2015.1131809.

Gutiérrez, X., F. Schiavi, and H. Keppler (2016), The adsorption of HCl on volcanic ash, *Earth Planet. Sci. Lett.*, *438*, 66–74, doi:10.1016/j.epsl.2016.01.019.

Hommel, R., C. Timmreck, and H. F. Graf (2011), The global middle-atmosphere aerosol model MAECHAM5-SAM2: Comparison with satellite and in-situ observations, *Geosci. Model Dev.*, *4*, 809–834, doi:10.5194/gmd-4-809-2011.

Klobas, J. E., D. M. Wilmouth, D. K. Weisenstein, J. G. Anderson, R. J. Salawitch (2017), Ozone depletion following future volcanic eruptions, *Geophys. Res. Lett.*, *44*, 7490–7499, doi:10.1002/2017GL073972.

Kremser, S. et al. (2016). Stratospheric aerosol—Observations, processes, and impact on climate, *Rev. Geophys., 54*(2), 278-335, doi: 10.1002/2015RG000511

Laakso, A., A.-I. Partanen, H. Kokkola, A. Laaksonen, K. E. J. Lehtinen, and H. Korhonen (2012), Stratospheric passenger flights are likely an inefficient geoengineering strategy, *Environ. Res. Lett.*, *7*(3), doi:10.1088/1748-9326/7/3/034021.

Mills, M. J., Schmidt, A., Easter, R., Solomon, S., Kinnison, D. E., Ghan, S. J., Neely, R. R., III, Marsh, D. R., Conley, A., Bardeen, C. G. and Gettelman, A. (2016), Global volcanic aerosol properties derived from emissions, 1990-2014, using CESM1(WACCM), *J. Geophys. Res. Atmos.*, *121*, 2332–2348, doi:10.1002/2015JD024290.

Morgenstern, O., P. Braesicke, F. M. O'Connor, A. C. Bushell, C. E. Johnson, S. M. Osprey, and J. A. Pyle (2009), Evaluation of the new UKCA climate-composition model—Part 1: The stratosphere, *Geosci. Model Dev.*, *2*, 43–57, doi:10.5194/gmd-2-43-2009.

Newhall, C., S. Self, and A. Robock (2018), Anticipating future Volcanic Explosivity Index (VEI) 7 eruptions and their chilling impacts. *Geosphere*, *14*, No. 2, 1-32, doi:10.1130/GES01513.1.

Niemeier, U., C. Timmreck, H.-F. Graf, S. Kinne, S. Rast, and S. Self (2009), Initial fate of fine ash and sulfur from large volcanic eruptions, *Atmos. Chem. Phys.*, *9*, 9043–9057, doi:10.5194/acp-9-9043-2009.

Pitari, G., V. Aquila, B. Kravitz, A. Robock, S. Watanabe, I. Cionni, N. De Luca, G. Di Genova, E. Mancini, and S. Tilmes (2014), Stratospheric ozone response to sulphate geoengineering: Results from the Geoengineering Model Intercomparison Project (GeoMIP), *J. Geophys. Res. Atmos.*, *119*, 2629–2653, doi:10.1002/2013JD020566.

Reid, J. S., Benedetti, A., Colarco, P. R., & Hansen, J. A. (2011). International Operational Aerosol Observability Workshop. *Bull. Amer. Meteorol. Soc.*, *92*(6), ES21–ES24, doi: 10.1175/2010BAMS3183.1

Ridley, D. A., Solomon, S., Barnes, J. E., Burlakov, V. D., Deshler, T., Dolgii, S. I., Herber, A. B., Nagai, T., Neely, R. R., III, Nevzorov, A. V., Ritter, C., Sakai, T., santer, B. D., Sato, M., Schmidt, A., Uchino, O. and Vernier, J. P. (2014). Total volcanic stratospheric aerosol optical depths and implications for global climate change, *Geophys. Res. Lett.*, *41*(22), 7763–7769, doi:10.1002/2014GL061541.

Robock, A. (2000), Volcanic eruptions and climate, *Rev. Geophys.*, *38*, 191-219, doi:10.1029/1998RG000054.

Robock, A., (1981), The Mount St. Helens volcanic eruption of 18 May 1980: Minimal climatic effect. *Science*, *212*(4501), 1383-1384, doi: 10.1126/science.212.4501.1383.

Salawitch, R. J., D. K. Weisenstein, L. J. Kovalenko, C. E. Sioris, P. O. Wennberg, K. Chance, M. K. W. Ko, and C. A. McLinden (2005), Sensitivity of ozone to bromine in the lower stratosphere, *Geophys. Res. Lett.*, *32*, L05811, doi:10.1029/2004GL021504.

Santer, B. D., et al. (2015), Observed multivariable signals of late 20th and early 21st century volcanic activity, *Geophys. Res. Lett.*, *42*, 500–509, doi: 10.1002/2014GL062366.

Sawamura, P., J. P. Vernier, J. E. Barnes, T. A. Berkoff, E. J. Welton, L. Alados-Arboledas, F. Navas-Guzmán, G. Pappalardo, L. Mona, F. Madonna, D. Lange, M. Sicard, S. Godin-Beekmann, G. Payen, Z. Wang, S. Hu, S. N. Tripathi, C. Cordoba-Jabonero, and R. M. Hoff (2012), Stratospheric AOD after the 2011 eruption of Nabro volcano measured by lidars over the Northern Hemisphere, *Environ. Res. Lett.*, *7*, doi:10.1088/1748-9326/7/3/034013.

Sekiya, T., K. Sudo, and T. Nagai (2016), Evolution of stratospheric sulfate aerosol from the 1991 Pinatubo eruption: Roles of aerosol microphysical processes, *J. Geophys. Res. Atmos.*, *121*, 2911–2938, doi:10.1002/2015JD024313.

Self, S. (2006), The effects and consequences of very large explosive volcanic eruptions, *Philosophical Transactions of the Royal Society of London A: Mathematical, Physical and Engineering Sciences*, *364*(1845), 2073–2097, doi:10.1098/rsta.2006.1814.

Sessions, W. R., Reid, J. S., Benedetti, A., Colarco, P. R., da Silva, A., Lu, S., et al. (2015). Development towards a global operational aerosol consensus: basic climatological characteristics of the International Cooperative for Aerosol Prediction Multi-Model Ensemble (ICAP-MME). *Atmospheric Chemistry and Physics*, *15*(1), 335–362, doi: 10.5194/acp-15-335-2015

Sheng, J.-X., D. K. Weisenstein, B.-P. Luo, E. Rozanov, A. Stenke, J. Anet, H. Bingemer, and T. Peter (2015), Global atmospheric sulfur budget under volcanically quiescent conditions: Aerosol-chemistry-climate model predictions and validation, *J. Geophys. Res. Atmos.*, *120*, 256–276, doi:10.1002/2014JD021985.

Tabazadeh, A., and R. P. Turco (1993), Stratospheric chlorine injection by volcanic eruptions: HCl scavenging and implications for ozone, *Science*, *260*, 1082–1086, doi:10.1126/science.260.5111.1082

Takigawa, M., Takahashi, M. and Akiyoshi, H. (2002), Simulation of stratospheric sulfate aerosols using a Center for Climate System Research/National Institute for Environmental Studies atmospheric GCM with coupled chemistry 1. Nonvolcanic simulation, *J. Geophys. Res.*, *107*(D22), 4610, doi:10.1029/2001JD001007.

Tanaka, T. Y., K. Orito, T. T. Sekiyama, K. Shibata, and M. Chiba (2003), MASINGAR, a global tropospheric aerosol chemical transport model coupled with MRI/JMA98 GCM: Model description, *Pap. Meteorol. Geophys.*, *53*(4), 119–138, doi:10.2467/mripapers.53.119.

Toohey, M., K. Krüger, and C. Timmreck (2013), Volcanic sulfate deposition to Greenland and Antarctica: A modeling sensitivity study, *J. Geophys. Res. Atmos.*, *118*, 4788–4800, doi:10.1002/jgrd.50428.

Tupper, A., J. S. Oswalt, and D. Rosenfeld (2005), Satellite and radar analysis of the volcanic-cumulonimbi at Mount Pinatubo, Philippines, 1991, *J. Geophys. Res.*, *110*, D09204, doi:10.1029/2004JD005499

van Noije, T. P. C., P. Le Sager, A. J. Segers, P. F. J. Van Velthoven, M. C. Krol, W. Hazeleger, A. G. Williams, and S. D. Chambers (2014), Simulation of tropospheric chemistry and aerosols with the climate model EC-Earth, *Geosci. Model Dev.*, *7*, 2435–2475, doi:10.5194/gmd-7-2435-2014.

Vernier, J. P., Thomason, L. W., Pommereau, J. P., Bourassa, A., Pelon, J., Garnier, A., Hauchecorne, A., Blanot, L., Trepte, C., Degenstein, D. and Vargas, F. (2011). Major influence of tropical volcanic eruptions on the stratospheric aerosol layer during the last decade, *Geophys. Res. Lett.*, *38*(12), L12807, doi:10.1029/2011GL047563.

Vernier, J. P., Fairlie, T. D., Deshler, T., Natarajan, M., Knepp, T., Foster, K., Wienhold, F. G., Bedka, K. M., Thomason, L. and Trepte, C. (2016), In situ and space-based observations of the Kelud volcanic plume: The persistence of ash in the lower stratosphere, *J. Geophys. Res.*, *121*, 11,104–11,118, doi:10.1002/2016JD025344.

Winson, A. E. G., F. Costa, C. G. Newhall, and G. Woo (2014), An analysis of the issuance of volcanic alert levels during volcanic crises, *J. Applied Volcanology*, *3*:14, doi:10.1186/s13617-014-0014-6.

Yu, P., Toon, O. B., Neely, R. R., Martinsson, B. G. and Brenninkmeijer, C. A. M. (2015), Composition and physical properties of the Asian Tropopause Aerosol Layer and the North American Tropospheric Aerosol Layer, *Geophys. Res. Lett.*, *42*(7), 2540–2546, doi:10.1002/2015GL063181.

Yukimoto, S., et al. (2011), *Meteorological Research Institute-Earth System Model Version 1 (MRI-ESM1)—Model description*, Technical Reports of the Meteorological Research Institute, No. 64, doi:10.11483/mritechrepo.64.